

General Disclaimer

One or more of the Following Statements may affect this Document

- This document has been reproduced from the best copy furnished by the organizational source. It is being released in the interest of making available as much information as possible.
- This document may contain data, which exceeds the sheet parameters. It was furnished in this condition by the organizational source and is the best copy available.
- This document may contain tone-on-tone or color graphs, charts and/or pictures, which have been reproduced in black and white.
- This document is paginated as submitted by the original source.
- Portions of this document are not fully legible due to the historical nature of some of the material. However, it is the best reproduction available from the original submission.

NASA TECHNICAL
MEMORANDUM

September 1974

NASA TM X-64823



MSFC SKYLAB APOLLO TELESCOPE MOUNT THERMAL
CONTROL SYSTEM MISSION EVALUATION

Skylab Program Office

NASA

*George C. Marshall Space Flight Center
Marshall Space Flight Center, Alabama*

(NASA-TM-X-64823) MSFC SKYLAB APOLLO
TELESCOPE MOUNT THERMAL CONTROL SYSTEM
MISSION EVALUATION (NASA) 63 p HC \$3.75

CSSL 14B

N74-32900

G3/14

Unclas
48531

1. REPORT NO. NASA TM X-64823	2. GOVERNMENT ACCESSION NO.	3. RECIPIENT'S CATALOG NO.	
4. TITLE AND SUBTITLE MSFC Skylab Apollo Telescope Mount Thermal Control System Mission Evaluation		5. REPORT DATE September 1974	6. PERFORMING ORGANIZATION CODE EP 44
		8. PERFORMING ORGANIZATION REPORT #	
7. AUTHOR(S) Uwe Hueter	9. PERFORMING ORGANIZATION NAME AND ADDRESS George C. Marshall Space Flight Center Marshall Space Flight Center, AL 35812		
12. SPONSORING AGENCY NAME AND ADDRESS National Aeronautics and Space Administration Washington, D. C. 20546		10. WORK UNIT NO.	11. CONTRACT OR GRANT NO.
		13. TYPE OF REPORT & PERIOD COVERED Technical Memorandum	
14. SPONSORING AGENCY CODE		15. SUPPLEMENTARY NOTES Prepared by Structures and Propulsion Laboratory/Engineering Analysis Division/ Thermal Engineering Branch	
16. ABSTRACT <p>The Skylab Saturn Workshop Assembly was designed to expand the knowledge of manned earth orbital operations and accomplish a multitude of scientific experiments. The Apollo Telescope Mount (ATM), a module of the Skylab Saturn Workshop Assembly, was the first manned solar observatory to successfully observe, monitor, and record the structure and behavior of the sun outside the earth's atmosphere. The Skylab mission began May 14, 1973, with launch of the Saturn Workshop Assembly and ended February 8, 1974, with the safe return of the SL-4 crew. The mission consisted of three manned periods lasting 28, 58, and 84 days, respectively.</p> <p>The ATM contained eight solar telescopes that recorded solar phenomena in X-ray, ultraviolet, white light, and hydrogen alpha regions of the electromagnetic spectrum. In addition, the ATM contained the Saturn Workshop Assembly's pointing and attitude control system, a data and communication system, and a solar array/rechargeable battery power system. This document presents the overall ATM thermal design philosophy, premission and mission support activity, and the mission thermal evaluation. Emphasis is placed on premission planning and orbital performance with particular attention on problems encountered during the mission. ATM thermal performance was satisfactory throughout the mission. Although several anomalies occurred, no failure was directly attributable to a deficiency in the thermal design.</p>			
17. KEY WORDS Skylab Apollo Telescope Mount Thermal Control Mission Evaluation		18. DISTRIBUTION STATEMENT Unclassified - Unlimited <i>James R. Lelbetter</i>	
19. SECURITY CLASSIF. (of this report) Unclassified	20. SECURITY CLASSIF. (of this page) Unclassified	21. NO. OF PAGES 61	22. PRICE NTIS

ACKNOWLEDGMENT

Although there were many individuals involved, the author would like to acknowledge especially all the members of the ATM Thermal Control System Mission Support Group for their contributions to this report. However, special acknowledgment is expressed to Messrs. John Chapter, Gary Johnsen, and Jim Hover, Martin Marietta Corporation, for compiling most of the data for this report, and to Mr. Howard Trucks, Chief, Spacecraft Thermal Design, for his valuable assistance in the preparation of this report.

TABLE OF CONTENTS

	Page
I. INTRODUCTION	1
II. VEHICLE DESCRIPTION	2
III. THERMAL DESIGN	5
A. Requirements	5
B. Philosophy	8
C. Design	10
IV. PREMISSION ACTIVITY	13
A. Test Program	14
B. Analytical Modeling	14
C. Predictions	19
V. MISSION SUPPORT	20
VI. MISSION THERMAL EVALUATION	21
A. Canister	22
B. Rack	29
C. Data Correlation	31
VII. OFF-NOMINAL CONDITIONS	38
A. Control Moment Gyro	38
B. Rate Gyros	40
C. Canister TCS Radiator	43
D. Solar Shield Absorptivity Degradation	45
E. Canister Pressure	46
F. Other Out-of-Limit Conditions	48
VIII. CONCLUSIONS	49
A. System Performance	49
B. Future Program Applications	49
IX. SUPPLEMENTARY DOCUMENTS	52

LIST OF ILLUSTRATIONS

Figure	Title	Page
1.	Skylab Saturn Workshop Assembly	3
2.	Apollo Telescope Mount	4
3.	Cutaway view of the ATM experiment canister	5
4.	ATM canister experiment locations	7
5.	Canister TCS	11
6.	Typical rack zone	13
7.	Skylab mission phase summary	22
8.	Skylab mission major event timeline	23
9.	Symbol definition for mission/test temperature tables	29
10.	Typical thermal cover temperature response.	35
11.	Canister correlation analysis for MD 39	37
12.	Predicted bearing temperatures during CMG number 1 failure	39
13.	Y-2 rate gyro over-temperature transients	41
14.	Rate gyro thermal model/test data correlation.	42
15.	Average absorbed radiator heat flux versus mission day	43
16.	Predicted/flight radiator average absorbed heat flux	44
17.	ATM canister solar shield solar absorptivity degradation	46
18.	Canister internal pressure profile after SL-1 launch.	47

LIST OF TABLES

Table	Title	Page
1.	ATM Experiment Requirements Pertinent to Thermal Control	7
2.	Thermal Design Deficiencies	9
3.	Environmental and Surface Properties	10
4.	ATM Thermal Test Program Development Tests	15
5.	ATM Mission Support Math Models	17
6.	ATM Data Sources	20
7.	ATM Out-of-Limit Temperature Summary	24
8.	ATM Canister Mission/Test Data Comparison	25
9.	ATM Canister TCS Orbital Performance Data	30
10.	ATM Rack Mission/Test Data Comparison	32

LIST OF ABBREVIATIONS AND SYMBOLS

AOS	Acquisition of Signal
APCS	Attitude and Pointing Control System
AS&E	American Science & Engineering
ATM	Apollo Telescope Mount
CBRM	Charger-Battery-Regulator Module
CM	Command Module
CMG	Control Moment Gyro
EPC	Experiment Pointing Control
EPEA	Experiment Pointing Electronic Assembly
EPS	Electrical Power System
EREP	Earth Resources Experiments Package
EVA	Extravehicular Activity
FAS	Fixed Airlock Shroud
FSS	Fine Sun Sensor
GMT	Greenwich Mean Time
GSFC	Goddard Space Flight Center
HAO	High Altitude Observatory
HCO	Harvard College Observatory
H α	Hydrogen Alpha
I&CS	Instrumentation and Communication System
IR	Infrared
J	Joule
K	Kelvin Degrees
kg	Kilograms
LOS	Loss of Signal
m	Meter
MD	Mission Day
min	Minutes
MDA	Multiple Docking Adapter
MOPS	Mission Operations Planning System
MSFC	George C. Marshall Space Flight Center
M/W	Methanol/Water
N	Newton
NASA	National Aeronautics and Space Administration
NRL	Naval Research Laboratory
OW	Orbital Workshop
PCM/DDAS	Pulse Control Modulator/Digital Data Address System
RGP	Rate Gyro Processor
s	Seconds

LIST OF ABBREVIATIONS AND SYMBOLS (Concluded)

SAM	Solar Array Module
SI	Solar Inertial Attitude
SL	Skylab
SM	Service Module
T	Temperature
TCS	Thermal Control System
TSU	Thermal Systems Unit
TV	Television
T/V	Thermal/Vacuum
XUV	Extreme Ultraviolet
ZLV	Vehicle Z-Axis Vertical Orientation
α_s	Solar Absorptivity
β	Angle Between Solar Vector and Orbital Plane
Δ	Change
σ	Standard Deviation

MSFC SKYLAB APOLLO TELESCOPE MOUNT THERMAL CONTROL SYSTEM MISSION EVALUATION

I. INTRODUCTION

The objectives of the Skylab missions were to study long duration effects on men and systems in earth orbit, to conduct various scientific experiments, and to observe the sun outside the earth's atmosphere. Skylab consisted of an Orbital Workshop (OW), an Airlock Module, a Multiple Docking Adapter (MDA), an Apollo Telescope Mount (ATM), and, during manned mission phases, a Command and Service Module. The spacecraft, launched May 14, 1973, by the National Aeronautics and Space Administration (NASA), remained operational until February 9, 1974, when the vehicle was placed in a gravity-gradient orientation and all systems were deactivated. During the mission, three different three-man crews visited the spacecraft for 28, 58, and 84 days, respectively. Two unmanned periods between manned periods lasted for 36 and 52 days, respectively. This document primarily discusses ATM, one module of the Skylab Assembly.

The objective for the ATM was to observe the sun outside the earth's atmosphere to provide high-resolution data of solar phenomena in X-ray, ultra-violet, white light, and hydrogen alpha regions of the electromagnetic spectra. Data were collected by eight solar telescopes housed in a cylindrical canister mounted with gimbal and roll rings on an octagonal structure that contained ATM's supporting equipment (e.g., power, data, and communication), as well as the Skylab's attitude and pointing control system. In addition, a sun shield and an x-shaped solar array were attached to the structure. The solar array generated all required electrical power for ATM and supplemented power to the Orbital Assembly.

Stringent pointing stability requirements of ATM telescopes resulted in the design of various thermal control schemes to prevent excessive thermal distortions. The telescopes were thermally controlled utilizing electrical heaters, thermal control coatings, and thermal isolation mounts in addition to being placed in a relatively constant temperature environment controlled by an active fluid thermal control system. Other electrical equipment, mounted on the octagonal support structure (rack), was passively controlled using insulation, thermal control coatings, thermal isolators, and thermostatically controlled heaters.

Prior to launching Skylab, ATM was subjected to various subsystem and system tests. The thermal test program contained ambient and thermal vacuum tests on subsystems and full scale models in addition to thermal vacuum testing of the flight and flight backup vehicles. During testing several design deficiencies, resulting from discrepancies between engineering data used in analyses and actual design and/or inherent weaknesses in the original design, were discovered and corrected.

ATM orbital thermal performance was excellent. Although several anomalies occurred during the 9-month mission, no failure was directly attributable to a deficiency in thermal design. Several components exceeded their temperature limits because of maneuvers not anticipated prior to flight. These maneuvers were required during early mission phases to prevent the Orbital Workshop's overheating since the meteoroid shield was lost during launch. In addition, excessive degradation of some surface coatings, along with some additional equipment failures, resulted in several items reaching their upper temperature limits.

Only thermal aspects of ATM, encompassing such items as thermal design, verification testing, premission and mission support activities, and mission thermal evaluation, are discussed in this document. The intent of the report is not to present all data gathered during the program but to emphasize the technical approach taken to achieve a viable system. Data are presented primarily to support resulting conclusions and recommendations. Sources of additional information concerning the Skylab mission are listed in Section IX. Supplementary Documents.

II. VEHICLE DESCRIPTION

Skylab, America's first experimental space station, was launched by a two-stage Saturn V vehicle. Skylab was a 90 720 kg vehicle containing four major modules (Fig. 1). The largest module, Orbital Workshop, was a modified third stage of the Saturn V vehicle. The hydrogen tank of this stage was outfitted with floors, dividers, and equipment to provide a manned laboratory and crew quarters. The crew performed various medical, scientific, and engineering experiments inside the Orbital Workshop. The second module, Airlock Module, served as a passageway between the Orbital Workshop and the Multiple Docking Adapter and as an airlock for astronaut extravehicular activity (EVA) to retrieve ATM film. The third module, Multiple Docking Adapter, was

attached to the Airlock Module and served as a docking port for the Apollo spacecraft that transported crews to Skylab from earth. The fourth module, ATM, primarily observed, monitored, and recorded the structure and behavior of the sun. ATM was also used for stellar and Comet Kohoutek observations.

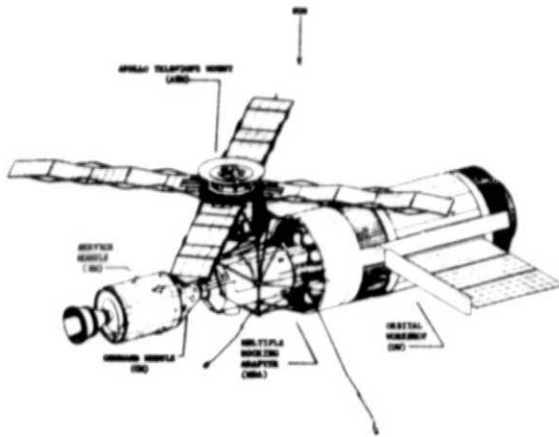


Figure 1. Skylab Saturn Workshop Assembly.

The ATM (Fig.2) was approximately 4.4 m wide (not including solar arrays), 3.6 m high, and weighed approximately 10 500 kg. The octagonal skeleton structure, known as the rack, supported the experiment canister and served as a mounting structure for more than 140 electrical and mechanical components. Electrical energy was provided by solar cells mounted on four wings deployed in an x-shaped arrangement from the rack. Energy available from solar cells was stored

in 18 nickel/cadium rechargeable batteries for use during earth shadow period. Major elements providing ATM pointing and control were control moment gyros (CMGs), control computers, an acquisition sun sensor, a star tracker, rate gyros, and a fine sun sensor. These components controlled Skylab's attitude and pointed ATM with an accuracy of ± 0.2 deg pitch and yaw and ± 10 arc min of roll. Fine pointing of the experiment canister was achieved through a gimbal and roll assembly that allowed relative motion of the canister to the rack of ± 2 deg in pitch and yaw and ± 120 deg in roll. Solar activity viewed by telescopes was displayed for astronaut monitoring at a control console located in the MDA. Using these displays and fine pointing control, the astronaut bore-sighted telescopes at interesting solar activity such as flares.

The canister was a 3.4 m long and 2.2 m diameter insulated cylinder housing eight solar telescopes, a fine pointing control system, several supporting electronic boxes, and a fluid loop thermal control system. A cutaway view of the canister is presented in Figure 3. All solar telescopes were mounted to an insulated cruiform type structure which divided the canister into four quadrants. The eight solar telescopes utilized to monitor and record events occurring on the sun were:

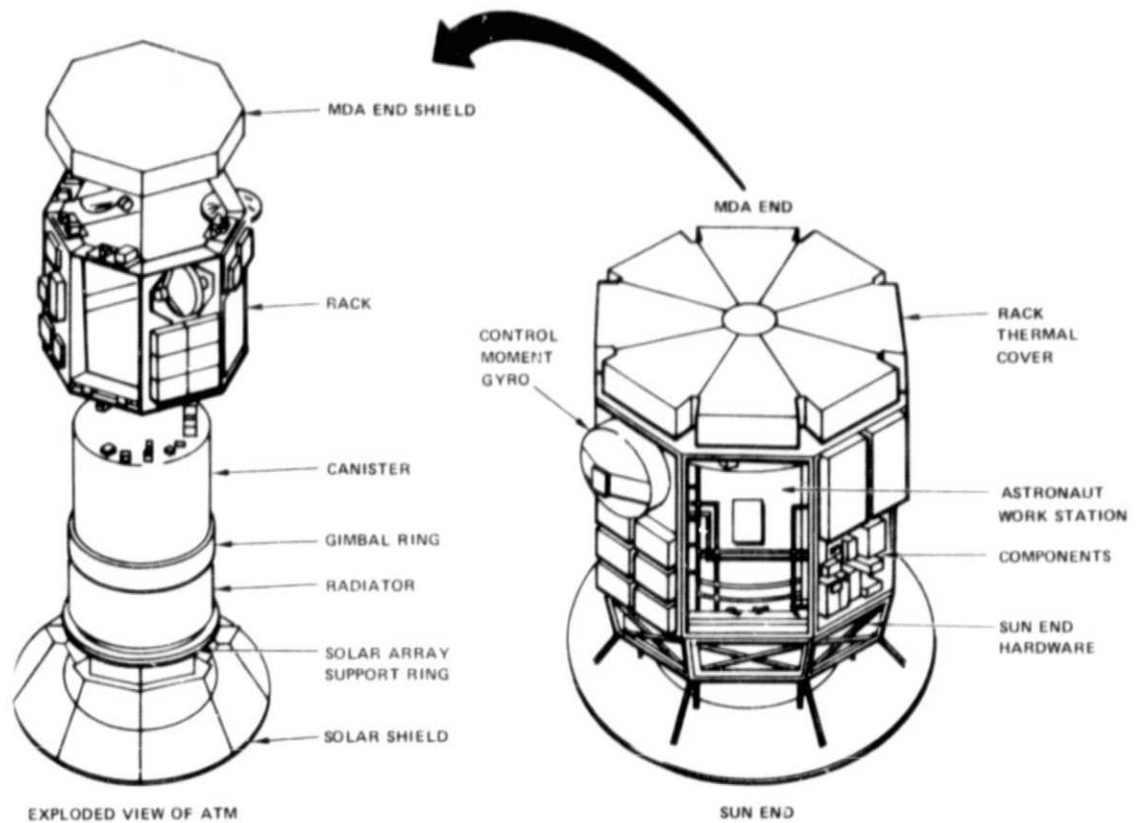


Figure 2. Apollo Telescope Mount.

1. High Altitude Observatory white light coronagraph telescope (S-052).
2. American Science and Engineering X-ray spectrographic telescope (S-054).
3. Harvard College Observatory ultraviolet scanning polychromator-spectroheliometer (S-055A).
4. Goddard Space Flight Center X-ray telescope (S-056).
5. Naval Research Laboratory (NRL) extreme ultraviolet spectroheliograph (S-082A).
6. NRL extreme ultraviolet spectrograph (S-082B).
7. Hydrogen alpha 1 telescope (H-Alpha 1).
8. Hydrogen alpha 2 telescope (H-Alpha 2).

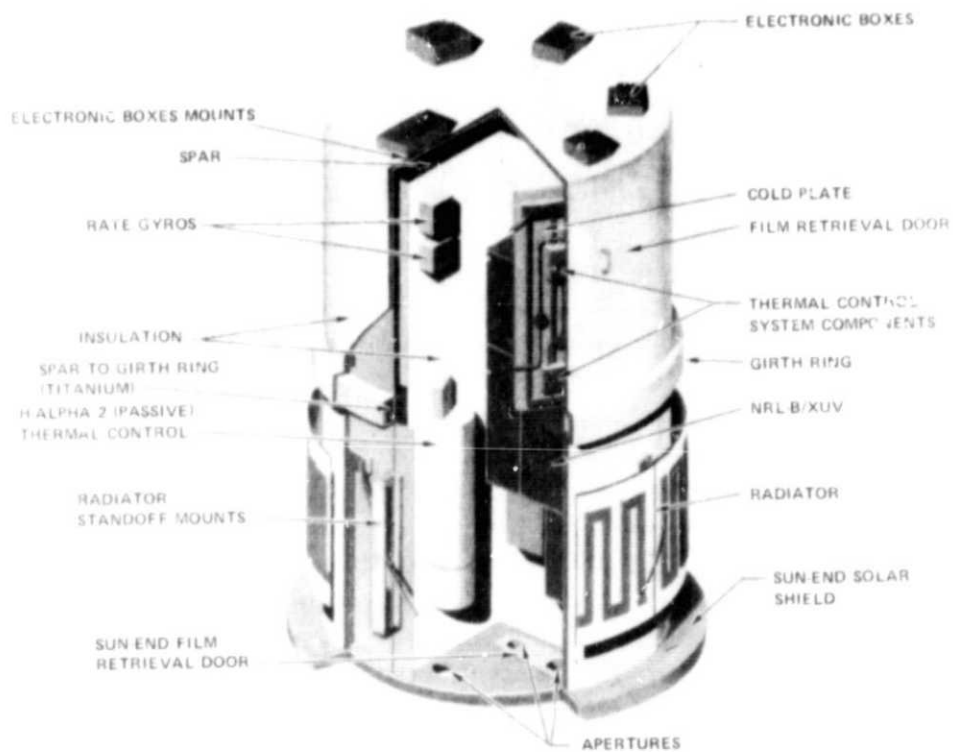


Figure 3. Cutaway view of the ATM experiment canister.

III. THERMAL DESIGN

A. Requirements

Mission requirements dictated that ATM thermal design be compatible with placing Skylab in an approximately circular 435 km earth orbit for an

8-month duration. The vehicle would remain solar oriented except for occasional maneuvers, earth resources experiments and stellar observations, that would not exceed two consecutive orbits.

Support electronic/mechanical components mounted on the rack had large operating temperature ranges. In general, the average operating temperature range for these components was between 253K and 323K. Two exceptions were charger-battery-regulator modules (CBRMs) (temperature range from 263K to 303K) and solar cells (temperature range from 208K to 373K). Additionally, all hardware used or touched by astronauts during EVA, e. g., retrieval of ATM film, etc., had maximum allowable temperature limits as follows:

1. Touch indefinitely for temperatures to 338K.
2. Light touch indefinitely for temperatures to 366K.
3. Light touch for 3 min for temperatures to 394K.

The ATM solar telescopes (experiments) were arranged inside the canister as shown in Figure 4. Because of stringent pointing stability requirements, close thermal control was required to prevent excessive thermal distortions. The experiments had two basic thermal requirements: (1) experiment case, or outer surface, temperature suitable as a heat sink for maintaining acceptable internal temperatures of mirrors, cameras, electronics, etc., and (2) stable mounting structure and thermal environment to minimize transient thermal gradients which could cause optical movement during data collection. Table 1 shows experiment requirements pertinent to thermal control. Experiments' response to canister wall temperature fluctuations plus the quantity of heat transferred by radiation from the telescopes to the canister walls dictated the following Thermal Control System (TCS) design requirements:

1. Canister fluid inlet temperature must not exceed the control limit of $283.2 \pm 1.7\text{K}$.
2. Maximum fluid temperature rise in the canister must not exceed 2.8K with an internal heat generation of 500 watts.
3. The radiator must be capable of rejecting 500 watts of energy at any time during the mission.

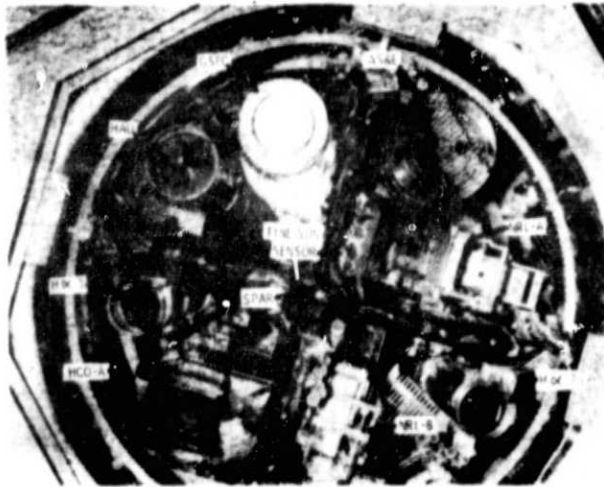


Figure 4. ATM canister experiment locations.

TABLE 1. ATM EXPERIMENT REQUIREMENTS PERTINENT TO THERMAL CONTROL

Experiment	Pointing Stability (arc sec)	Exposure Time (min)	Experiment Power (W)			
			Avg. Elec.	Solar Minus Rerad.		Avg. Total
				Max.	Avg.	
GSFC	± 2.5	1.6	32	37	27	59
AS&E	± 2.5	5.0	44	19	11	56
HCO-A	± 2.5	15.0	55	28	20	75
HAO	± 5	16.0	23	14	10	33
NRL-A	± 2.5	5.0	21	4	3	24
NRL-B & XUV	± 2.5	15.0	42	4	3	45
H-Alpha 1	± 0.5	15.0	14	2.5	1.5	15.5
H-Alpha 2	± 0.5	15.0	10	2.5	1.5	11.5

B. Philosophy

Thermal design complexity and stringent telescopes thermal control requirements resulted, early in the program, in the decision that the ATM program utilize a comprehensive analytical approach supported by a thorough thermal vacuum test program. Previous experience on other programs had shown that either a purely analytical or test approach was unrealistic. The Ranger program, relying heavily upon analysis, and the Mariner program, primarily utilizing thermal vacuum test data, both experienced flight temperatures significantly different from expected values. The weaknesses in utilizing only an analytical or test approach are shown in Table 2.

Initial analytical studies were conducted with simplified models to allow tradeoffs involving experiment requirements, mission requirements, and candidate designs which resulted in sound design concepts capable of meeting mission objectives. Chosen concepts were incorporated into test articles during early developmental thermal vacuum test programs. Data from these tests were utilized to (1) support construction of detailed computerized analytical models, and (2) identify design deficiencies early in the development phase. After detailed analytical models had been constructed, temperature predictions were made for the ATM during all major mission phases. Analyses were conducted for maximum and minimum environments to assure that no components exceeded their respective temperature limits. The thermal analyses utilized environmental and optical property data based on a $\pm 3\sigma$ variation, as shown in Table 3.

Three full-scale ATM thermal vacuum tests were conducted. The first utilized a Thermal Systems Unit (TSU) where most components were thermal simulators of flight hardware. Since the flight backup and flight ATMs were equipped with only limited thermal instrumentation, the TSU test was the prime source of detailed thermal behavior data for the ATM. Thus, the primary objective of the TSU test program was to verify analytical techniques utilized to develop detailed analytical models. To achieve verification of analytical techniques, tests were conducted with known, analytically predictable, test environments which, in many cases, did not duplicate the anticipated space environments. The requirement of providing a known environment resulted in emphasis on design, calibration, and operation of an environmental simulator. However, by establishing known test environments which duplicated, as closely as possible, maximum and minimum anticipated flight environments, limited acceptance or qualification tests were also performed. These tests were planned to force design weaknesses (if they existed) so that the potential failure points and the type of failure were known. Consequently, major design changes were eliminated for the flight article.

TABLE 2. THERMAL DESIGN DEFICIENCIES

Analytical Approach Only	Test Approach Only
<ol style="list-style-type: none"> 1. Simplifying engineering assumptions must be made to obtain a solvable mathematical model. 2. Assumptions increase with increased complexity 3. Excessive penalties possible, e.g., weight, volume, and power, due to conservative approach. 4. Analyses accuracy dependent upon design parameters and physical property values accuracies. 	<ol style="list-style-type: none"> 1. System response to nontested elements, e.g., solar arrays, or added elements, e.g., support structures, may not be known. 2. Exact orbital environment cannot be duplicated in thermal vacuum testing because of vacuum chamber limitations. 3. Costs prohibit thermal vacuum testing of all flight conditions. 4. Failure modes and/or parametric analysis cannot be investigated extensively in thermal vacuum tests. 5. Thermal vacuum testing does not permit flexibility to incorporate late design and/or mission changes. 6. Instrumentation limitations prohibit temperature measurements of every component on large spacecrafts. 7. Unscheduled system operation or orientation during mission cannot be assessed accurately.

TABLE 3. ENVIRONMENTAL AND SURFACE PROPERTIES

Parameter	Hot Case	Nominal Case	Cold Case
Solar Constant (J/s-m ²)	1441	1353	1265
Albedo	0.42	0.30	0.18
Planetary Emission (J/s-m ²)	279	237	194
White Paint (S-13G)			
Ultraviolet Absorptivity	0.50	0.35	0.20
Infrared Emissivity	0.90	0.90	0.90
Black Paint			
Ultraviolet Absorptivity	0.90	0.90	0.90
Infrared Emissivity	0.90	0.90	0.90

C. Design

The wide variation of thermal design requirements for the telescopes and equipment resulted in three distinct thermal designs. First, the experiments operated over very limited temperature ranges where an active thermal control system was required to provide a nearly constant radiation environment. Second, electrical heaters, insulation, and thermal control coatings closely maintained correct temperatures of individual telescopes to reduce thermal distortions that would adversely affect pointing accuracy and stability. Third, rack components operated over large temperature ranges where passive thermal control supplemented by auxiliary, thermostatically controlled heaters provided adequate control.

1. Canister. The canister, an insulated cylinder shielding the eight telescopes from the space environment, provided a uniform and nearly constant internal environment and served as a stable telescope-mounting platform. All telescopes were mounted on an isolated structure (referred to as the spar) that divided the canister interior into four quadrants. The spar was supported by a girth ring that connects to the gimbal system. Spar thermal isolation was required to minimize spar temperature gradients that would cause optical misalignment. Thermal isolation was achieved by using low-conductance mounts

at the telescopes/spar and the spar/girth ring interface. In addition, the entire spar was manufactured from aluminum and encapsulated with multilayer insulation. The entire canister exterior was encapsulated with multilayer insulation to thermally isolate the canister cold plates from the external environment. Major canister heat shorts were 6 film retrieval doors, 1 telescope access door, 10 sun-end aperture doors, and standoffs for the thermal control system radiator panels. The canister sun-end had a 0.25 m overhang to prevent solar energy impingement directly on the radiator panels mounted to the exterior sun-end sidewall.

The canister's interior walls, painted black to minimize reflections and maximize radiative coupling between the telescopes and cold plates, were maintained at a nearly constant temperature by a closed-loop fluid, heat-transport system (Fig. 5). Heat dissipated by the telescopes was absorbed by

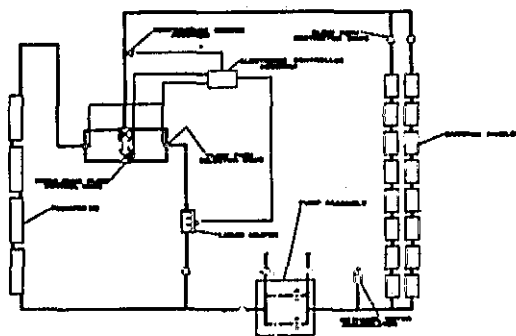


Figure 5. Canister TCS.

the canister wall cold plates. transferred to the radiator by the fluid loop, and then rejected to the external environment. The thermal control system contained 16 cold plates, 4 radiator panels, a pump package, an accumulator, an in-line heater, a mixing valve, a fluid filter, associated valves, and connective tubing. The working fluid was methanol/water (M/W) (80/20 percent by weight) with a nominal system flow of 0.107 kg/s. The fluid exited the pump and was filtered and split into two parallel paths,

radiator, and heater legs. A mixing valve proportioned flow through the legs and was positioned by signals from an electrical control assembly that monitored canister inlet temperature. The electrical control assembly also energized the in-line heater if the mixed temperature dropped below 281.90K. The flow was split into equal flowrates before entering the cold plates and flowed in parallel through the two canister halves. Flow leaving the canister halves mixed and then passed an accumulator before entering the pump.

Separate thermal design of each telescope was required to satisfy individual pointing stability requirements and maintain focal lengths within specified tolerances. To meet these objectives, temperature gradients in all telescopes were minimized by the following thermal control techniques:

1. Thermal isolation between telescopes and mounting spar forced radiation heat transfer to control energy exchange between the telescopes and their heat sink (canister cold plates).
2. Thermal coatings and insulation were utilized to control different heat dissipation rates.
3. High conductance material used in construction of instrument housings reduced temperature gradients.
4. Thermostatic heaters corrected thermal disturbances.

Heater systems for telescopes included standoff heaters and integral heaters. The standoff heater concept utilized low-capacitance, thermostatically controlled radiation shields over the instrument case. Low shield capacitance and high heater power caused high frequency shield temperature cycles which were successfully damped by the instrument's higher thermal capacity to maintain relatively constant case temperatures. These on/off heaters had fixed set point temperatures controlled to $\pm 0.28\text{K}$. Integral heaters utilized either an on/off type, or a proportional type of power control. Two telescopes had a very low heat dissipation rate that allowed the use of a gold coating whose low emissivity isolated the telescopes from external temperature variations, thus eliminating the need for an active thermal system.

2. Rack. The 2.8 by 4.0 m octagonal rack structure surrounded and supported the canister housing the telescopes. Also mounted to the rack were electrical and/or mechanical components that compose the power, telemetry, and pointing and control systems. Approximately 2500 watts of heat dissipated by components were rejected to space by passive methods utilizing surface coatings, thermal isolation mounts, insulation, radiation shields, and thermal coupling. The passive thermal design maintained satisfactory component temperatures under all anticipated orbital conditions.

The philosophy underlying the rack thermal control concept was first to eliminate any "hot case" operational conditions that would cause a component to exceed its maximum allowable temperature limit; for example, by mounting the component to a radiating surface with good thermal contact. Second, components operating below their allowable minimum temperatures were (1) individually and/or collectively thermally isolated from the rack structure with fiberglass and titanium bracketry, (2) covered with thermal shields to reduce radiation heat losses, and (3) insulated until predicted component temperatures

approached their maximum allowable temperatures. Finally, auxiliary, thermostatically controlled heaters were added to components that would operate below their minimum temperature during the "cold case." Thus, rack thermal control design stressed maximum use of passive thermal control and minimized heater power requirements. A typical rack component mounting bay is shown in Figure 6. The following significant thermal requirements were incorporated into the design:

1. ATM surface exposed to external environments were painted white to reduce heating.

2. Thermal shields protected components with low-power densities from cold environments. These shields were covered with varying thicknesses of multilayer insulation to control heat losses.

3. All major mounting panels, except those containing high-heat dissipating components such as batteries, were isolated from the rack structure and covered with multilayer insulation.

4. Components were located so that power distribution in major zones around the rack sides was reasonably uniform.

5. Components dissipating heat at high rates were mounted on external panels.

6. A rack-mounted sun shield prevented continuous direct solar impingement on rack components.

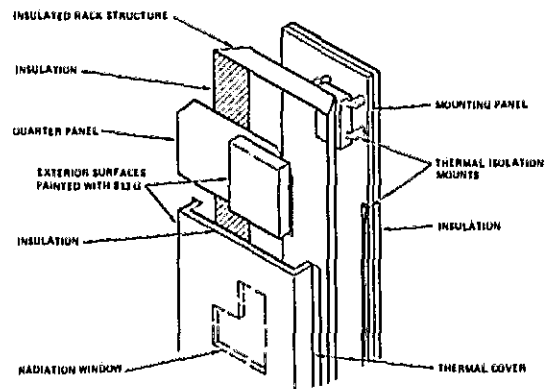


Figure 6. Typical rack zone.

IV. PREMISSION ACTIVITY

Prior to launch of Skylab, ATM's thermal behavior was mathematically analyzed and hardware was subjected to various tests, both ambient and thermal vacuum, to assure design adequacy and correct mathematical representation of actual hardware. Finally, mission predictions were made for most anticipated orbital operations and various contingency and failure modes.

A. Test Program

An extensive ATM test program, ranging from six development tests to four full-scale thermal vacuum tests, was conducted between 1967 and 1972. The six ATM development tests, their respective objectives, and test results summary are shown in Table 4.

The first full-scale system test was conducted on the canister in a small vacuum chamber at MSFC to obtain early performance data on the canister TCS and experiments. Early in the test an instability, fluctuating flow and pressure, was discovered in the TCS. A breadboard test program ascertained that the major instability contributors were unbalanced fluid forces, excessive time constants, and valve mechanical characteristics.

The first full-scale thermal vacuum test of the complete ATM module was the TSU, a flight type structure utilizing thermal simulators for most components. The primary purpose of the test was to verify overall thermal system design, prior to subjecting flight hardware to anticipated flight conditions. Therefore, the TSU was heavily instrumented (compared to the flight backup and flight vehicle) to provide detailed thermal data when subjected to steady-state and transient orbital heat fluxes simulating extreme hot and cold conditions, in addition to certain failure tests (e. g., TCS failure).

The backup flight article, or prototype vehicle, was tested in the same vacuum facility as the TSU. The configuration and test program were basically identical except that all components were flight hardware. Test results verified overall satisfactory thermal system performance; however, 18 components were not maintained within their proper operating temperature range. Deficiencies, such as improper heater size, poor insulation application, low component power dissipation, and component failures, were all corrected on the flight vehicle.

The ATM flight vehicle thermal vacuum test, although similar to the prototype test, was not as extensive. Test results verified that design changes made after the prototype tests were satisfactory and overall vehicle thermal performance was adequate.

B. Analytical Modeling

Evaluation of the ATM hardware thermal compatibility resulted in the development of several mathematical models. These used the lumped-parameter nodal analysis technique in conjunction with standard thermal analyzer computer

TABLE 4. ATM THERMAL TEST PROGRAM DEVELOPMENT TESTS

Test	Objective	Results
Spar Stability	Evaluate Stability for Anticipated Temperature Gradient Extremes	Maximum Deflection 0.5 arc sec
Pump Jitter	Evaluate Effect of Pump Operation on ATM Experiments	Pump Vibrations Easily Isolated
Canister and Radiator Pressure Drop	Establish Flow Distribution, Determine Pressure Losses, Evaluate Fabrication Techniques	Pressure Loss, Within Allowable Limits; Verified Analytical Model for Pressure Loss Calculations
Radiator Bond/Coolant Compatibility	Determine Long Term Effect of Coolant fluid on Bonding Agent	System Utilizes Welding
Canister Quadrant	Verify Experiment Package Thermal Control Concept, Verify Insulation Performance, Early Experience with ATM Thermal Vacuum Testing	Identified Heater Design Changes
Rack Quadrants	Determine Component Temperature Extremes, Relocate and/or Modify Components as Required, Verify Math Model Techniques	Identified Insulation Pattern Changes, Identified Heater Design Changes

programs. The scope of this report has been limited to thermal math models used in direct support of the Skylab mission to perform premission predictions or to generate analytical studies during the mission.

The development of the thermal models resulted in three levels of detail:

<u>Model Level</u>	<u>Description</u>
1. System	Emphasis on systems performance, single thermal model to determine interactions between subsystems or components
2. Subsystem	Thermal interactions of several components that perform a specific function
3. Component	Calculate detailed temperature gradients and temperatures for single components

Thermal models included three systems, four subsystems, and seven component level simulations as described in Table 5. The table includes model level, construction/utilization times, number of nodes and construction rationale. These models provided ATM baseline thermal analysis capability and were used to support thermal vacuum testing, premission analyses, real-time mission analyses, and final mission thermal evaluation. Rapid analysis turnaround during the mission was provided by component level math models programmed for a readily accessible small computer. The large system models required a Univac 1108 or CDC 6600 type computer where turnaround time hampered prompt response for mission support.

The ATM environmental models provided total absorbed thermal fluxes for surfaces on the ATM rack structure and canister radiator. The total external flux absorbed by a spacecraft external surface consisted of heat flux from natural bodies (earth, sun) and infrared (IR) flux from surrounding structures. Absorbed fluxes were calculated at orbital intervals of 30 deg requiring 20 min per orbit point computer time (CDC 6600 or Univac 1108 computer) for a solar oriented orbit.

The rack thermal model described the rack structure, components, and canister gimbal rings utilizing 1305 nodes and 10 591 radiation and conduction couplings. The model was capable of steady-state and transient thermal simulations for various flight conditions. Environmental conditions for various

TABLE 5. ATM MISSION SUPPORT MATH MODELS

Id No.	Name	Model Level	Construction		Utilization		No. Nodes	Construction Rationale
			Pre-mission	During Mission	Pre-mission	During Mission		
1.	Rack	System	X		X	X ^a	1305	T/V test performance mission studies, heater duty cycles
2.	Canister		X		X	b	1391	T/V test performance mission studies, experiment duty cycles
3.	ATM Environments	Subsystem	X		X		138/309 ^c	ATM absorbed heat flux for T/V testing, analysis
4.	Liquid TCS		X		X		198	Mission studies, flowrates, pressure drops, heat loads
5.	Rack/Canister Interface		X		X		350	Mission studies for components between canister and rack
6.	Canister Gimbal System	Component	X		X		168	Temperature gradients in gimbal system
7.	Solar Array		X		X		131/346 ^c	Solar array and rack heat fluxes, solar array temperatures
8.	Solar Cell	Component	X		X		220	Cell temperatures due to failure of adjacent cells
9.	CMG		X		X	X	61	Calculate temperature gradients, bearing duty cycle

TABLE 5. (Concluded)

Id No.	Name	Model Level	Construction		Utilization		No. Nodes	Construction Rationale
			Pre-mission	During Mission	Pre-mission	During Mission		
10.	CBRM		X		X		478	Detailed battery temperature distribution
11.	Film Magazine		X		X	X	7	Calculate temperature history for exposed and unexposed magazines during EVA
12.	Rate Gyro			X		X	76	Assist identification of failure modes of flight rate gyros
13.	Rate Gyro Six-Pack			X		X	86	Calculate six-pack temperatures for MDA environment
14.	Quartz Microbalance		X			X	18	Temperature limit analysis

- a. Rate gyro analyses; steady-state and transient correlation with flight data for SL-2/SL-3.
- b. Steady-state and transient correlation with flight data for SL-2/SL-3.
- c. Heat rate surface model/thermal analyzer model.

beta (β) angles and external heat loads (varying from cold to hot), as well as various component power dissipations, were easily simulated by using program operational flags. Steady-state analyses required approximately 7 min of computer time utilizing a CDC 6600 or Univac 1108 computer. Transient analyses required approximately 30 min of computer time per orbit.

The ATM canister thermal model included the canister structure, experiments, liquid TCS, and spar. The model had 1391 nodes and 11 119 radiation and conduction couplings. The primary purpose of the model was to verify component and subsystem thermal compatibility. Major emphasis, 54 percent of the nodal allocation, was given to the eight experiments housed within the canister. The canister model permitted steady-state and transient thermal simulations generally requiring 10 min of computer time for steady-state analyses and 40 min to simulate one orbit during transient analysis on a CDC 6600 or Univac 1108 computer. Provisions were included to vary environmental conditions, experiment component operational nodes, and power levels, as well as logic controlling event timing, temperature initialization, problem storage, and data storage for plotted output. Analysis output included nodal temperatures and experiment TCS duty cycles.

C. Predictions

ATM mission support thermal models described in Section IV-B were all utilized to generate temperature predictions for various flight operational modes. Generally these studies included "hot" and "cold" conditions. Thermal coatings and environmental fluxes, as described in Table 3, in addition to various operational modes were used to establish the maximum and minimum thermal conditions. Because of the relatively large variations in temperatures of the externally mounted rack components, assessment of nominal conditions were also made. These predictions, along with test data, were used to generate parametric data relating flight temperature measurements to uninstrumented component temperatures.

Transient heat flux and temperature predictions for various β angles, encompassing maximum and minimum environmental conditions, formed the baseline of anticipated vehicle performance. Temperature predictions were also performed for orbital insertion/activation, operational and selected off-solar attitudes.

Twenty-one premission contingency studies were also performed based on probable failure modes for the ATM. These studies were chosen to enable rapid thermal evaluation in the event of component and/or system failures. The majority of these studies were performed using the system and subsystems level math models.

V. MISSION SUPPORT

Approximately 6 man-years were expended for ATM thermal support during the 9-month Skylab mission. ATM thermal personnel were assigned monitoring responsibilities of ATM parameters to assure proper thermal conditions for all ATM components. To assess ATM thermal status, approximately 42 percent of all temperature and pressure measurements were plotted continuously from real-time data for the entire mission. Continuous data plotting allowed determination of long and short term trends which developed, thereby alerting thermal personnel to take appropriate corrective actions.

ATM data available during the Skylab mission for monitoring and analysis is shown in Table 6. The majority of temperature and pressure measurements were not recorded by the onboard tape recorder; therefore, data could only be monitored while Skylab was over ground stations. Since ground coverage was not continuous [some orbits had up to 1 hour time lapses between station passes (the orbital period was 94 min)], it was possible to miss data during some major events, e.g., failure of one ATM CMG. Real-time data, used for day-to-day monitoring of the ATM thermal status, was available in special preprogrammed formats on TV monitor and in hard copy format. Meters and event lights were used by console operations for monitoring significant parameters. The Mission Operations Planning Support (MOPS) program was addressed to obtain time histories of data up to 48 hours. In addition to the above data sources, data books, microfilm, and magnetic tapes were available within 3 to 7 days for all data. The magnetic tapes were direct input sources for analytical thermal models used in the postmission analysis.

TABLE 6. ATM DATA SOURCES

<p><u>Real Time Data</u></p> <p>Data TV (Primary Data Source for Real Time Monitoring) Strip Charts (Parameters Monitored Usually Attributed to an Anomaly) Meters (Canister TCS Data) Event Light (Canister TCS Status)</p>
<p><u>Near-Real Time Data (3 → 48 Hours Old)</u></p> <p>MOPS - Mission Operations Planning Support (Primary Data Source for Establishing Time History of Recently Occurring Event)</p>
<p><u>Delayed Time Data (3 → 7 Days Old)</u></p> <p>Hard Copy Data Books (Mission and Postmission Evaluation) Microfilm (Postmission Evaluation) Magnetic Tape (Input to Analytical Models)</p>

The problems that developed early in the Skylab mission required that the vehicle be oriented in attitudes for which the ATM thermal system was not originally designed. Therefore, real-time analysis was conducted to determine the most thermally acceptable off-axis orientation to satisfy ATM thermal requirements and still maintain other Skylab hardware within acceptable temperatures. Thermal analyses were also conducted to determine the temperatures of a proposed solar array module (SAM) that was to have been brought to Skylab by the crew to supplement the electrical power. However, the effort was cancelled after the first crew freed the solar array wing on the Orbital Workshop. Extensive thermal analyses were conducted to determine causes of rate gyro and CMG failures, in addition to analyses conducted on the rate gyros installed in the MDA to replace the failed ATM rate gyros. Other analyses, e.g., film camera temperatures during EVA and degradation of surface paints, were also conducted. Most of the analyses utilized component models rather than the system models since fast computer turnaround time was required. The majority of this effort was directly related to specific component failures rather than overall vehicle performance. However, at the completion of each manned mission, typical hot and cold environment analyses were conducted to compare flight data with analytical predictions.

VI. MISSION THERMAL EVALUATION

The Skylab mission duration was 271 days, as depicted in Figure 7. A major event timeline is presented in Figure 8 with mission milestones and off-nominal conditions identified. An evaluation of ATM thermal performance was made to (1) determine if design objectives were met, (2) describe thermally significant events and mission impact, and (3) measure effectiveness of thermal vacuum testing and analytical tools. Performance of ATM's thermal control system was satisfactory throughout the Skylab mission. No thermal design inadequacies were identified nor were there any thermally-induced equipment failures. With few exceptions, ATM's thermal performance remained within allowable limits although the vehicle was oriented in orbital attitudes exceeding design specifications. ATM data show that 15 key temperature measurements violated allowable limits at times during the mission (Table 7). As indicated, these out-of-limit temperature conditions were attributed to off-attitudes, component failures, thermal coating degradation, and equipment operational changes. None of these out-of-limit temperatures seriously impacted ATM operation or objectives. Section VII of this report presents a detailed discussion of off-nominal conditions affecting ATM thermal control. Comparisons between mission data and ground thermal vacuum test data indicated that the flight

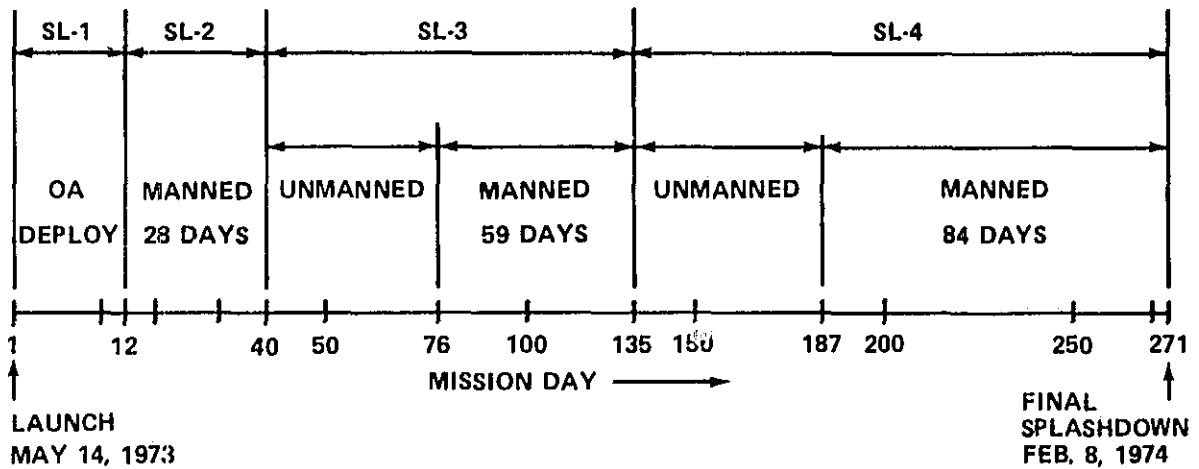


Figure 7. Skylab mission phase summary.

thermal environment was within the extremes imposed in test, with the exception of the ATM radiator zones which exceeded maximum anticipated environments. The only off-nominal thermal control condition during the mission was the degradation rate of S-13G paint on the solar shield. Although this caused several minor out-of-limit temperatures late in the mission, the condition had no significant impact. The mission data and a general evaluation of ATM thermal performance are presented in the following subsections.

A. Canister

Thermal control of ATM experiments and components within the canister was satisfactory. The maximum and minimum temperatures during the manned mission when experiments were active are given in Table 8. Temperature scale symbols are identified in Figure 9, p. 29. Flight data are compared with test data and operational temperature limits to indicate out-of-limit conditions. In general, mission temperature ranges are wider than those in ground testing because maximum mission temperatures occurred late in the mission when solar shield temperatures were abnormally high, and minimum mission temperatures were generally associated with early mission activity when experiments operated at standby power profiles lower than exercised during ground tests. Generally, mission data for the canister/spar structures were not bounded by ground test data because sun-end plate temperatures were higher during flight because of degraded paint on the solar shield (see Section VII-D).

REPRODUCIBILITY OF THE ORIGINAL PAGE IS POOR

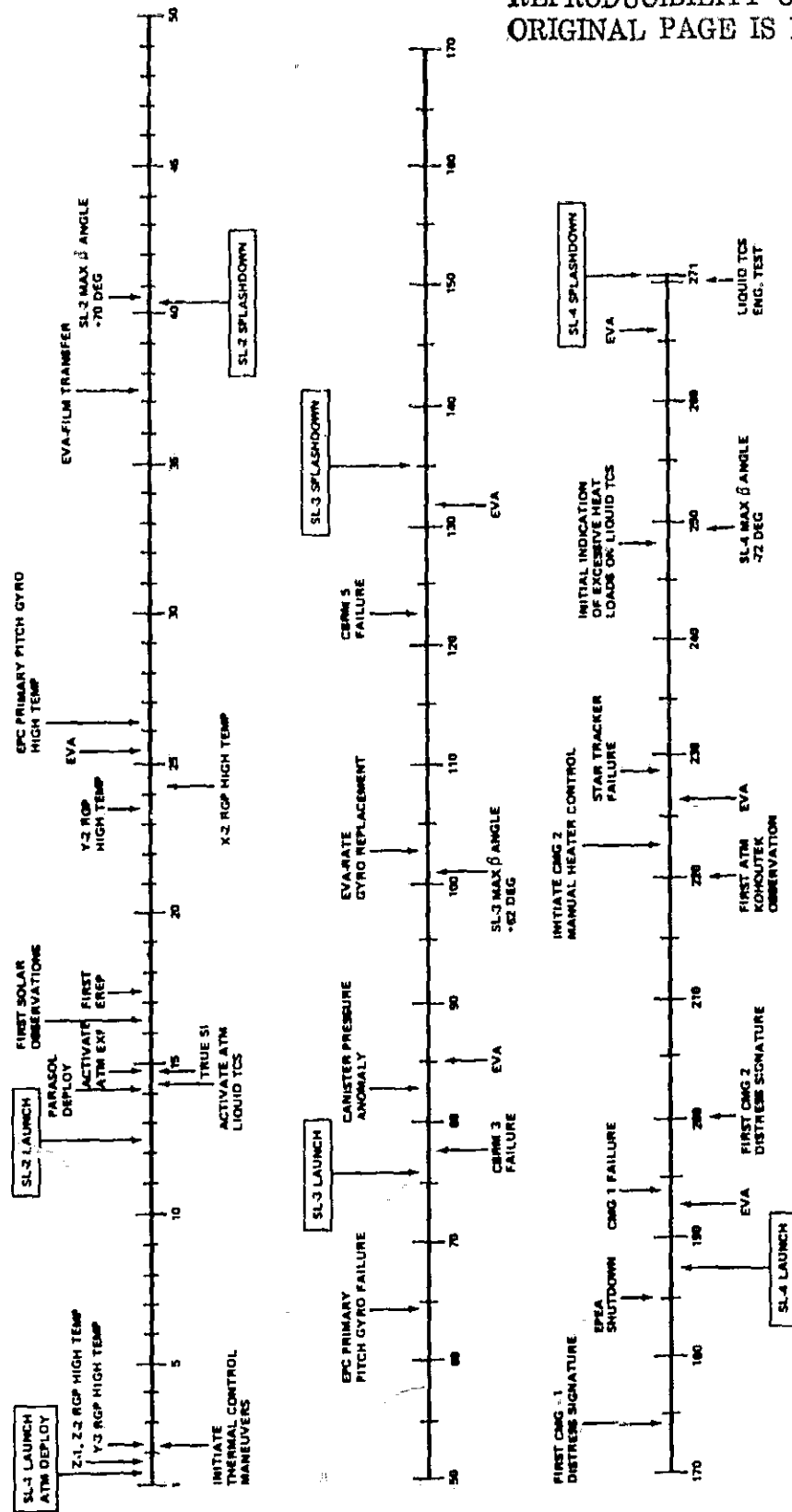
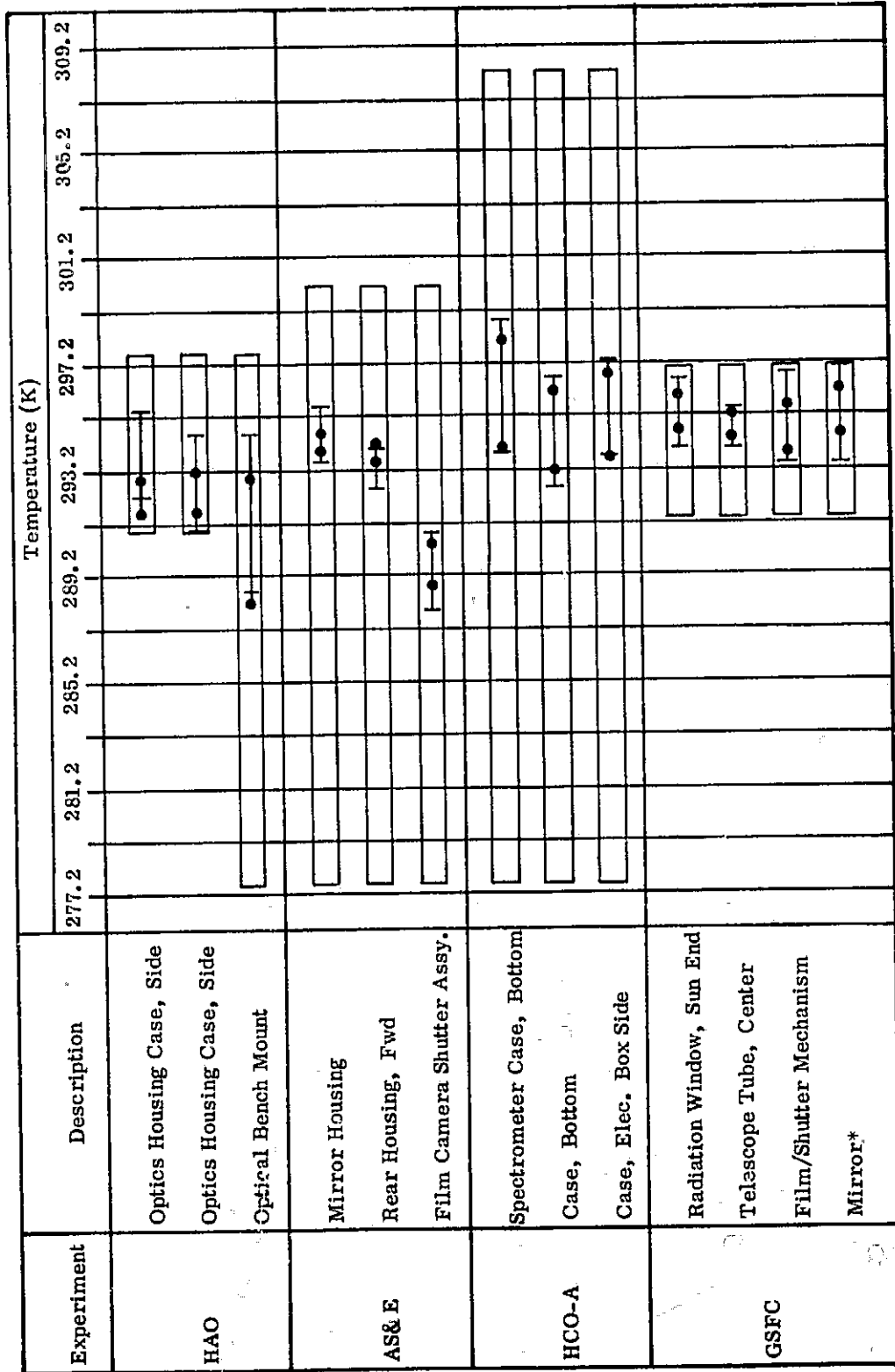


Figure 8. Skylab mission major event timeline.

TABLE 7. ATM OUT-OF-LIMIT TEMPERATURE SUMMARY

Component	Location	Operational Temperature Limits (K)	Out-of-Limit Temperature (K)	Cause of Out-of-Limit Condition
GSFC Mirror	Canister	291.5 - 297.1	297.3	Coating degradation
Pri Pitch Rate Gyro		339.9 - 341.9	Off-Scale-High	Electrical failure
Spar, Sun-End Inboard		283.1 - 294.2	294.3	Coating degradation
H-Alpha 1 Rear Tube		288.7 - 299.8	288.2	Operational change
H-Alpha 2 Rear Tube		288.7 - 299.8	287.5	Operational change
CMG 1 Bearing 1	Rack	288.8 - 328.2	355.6	Bearing failure
CBRM 17		263.2 - 303.2	303.3	Off-attitude
ATM Solar Panel		208.2 - 373.2	201.2	Off-attitude
ATM Solar Panel		208.2 - 373.2	207.2	Off-attitude
Z-1 Rate Gyro		339.9 - 341.9	Off-Scale-High	Electrical failure
Tape Recorder		273.2 - 303.2	303.7	Off-attitude
X-2 Rate Gyro		339.9 - 341.9	Off-Scale-High	Electrical failure
Y-2 Rate Gyro		339.9 - 341.9	Off-Scale-High	Electrical failure
Z-2 Rate Gyro		339.9 - 341.9	Off-Scale-High	Electrical failure
Y-3 Rate Gyro		339.9 - 341.9	Off-Scale-High	Electrical failure

TABLE 8. ATM CANISTER MISSION/TEST DATA COMPARISON



*Mission data shown for SL-3 & SL-4 only; not monitored prior to SL-3

TABLE 8. (Continued)

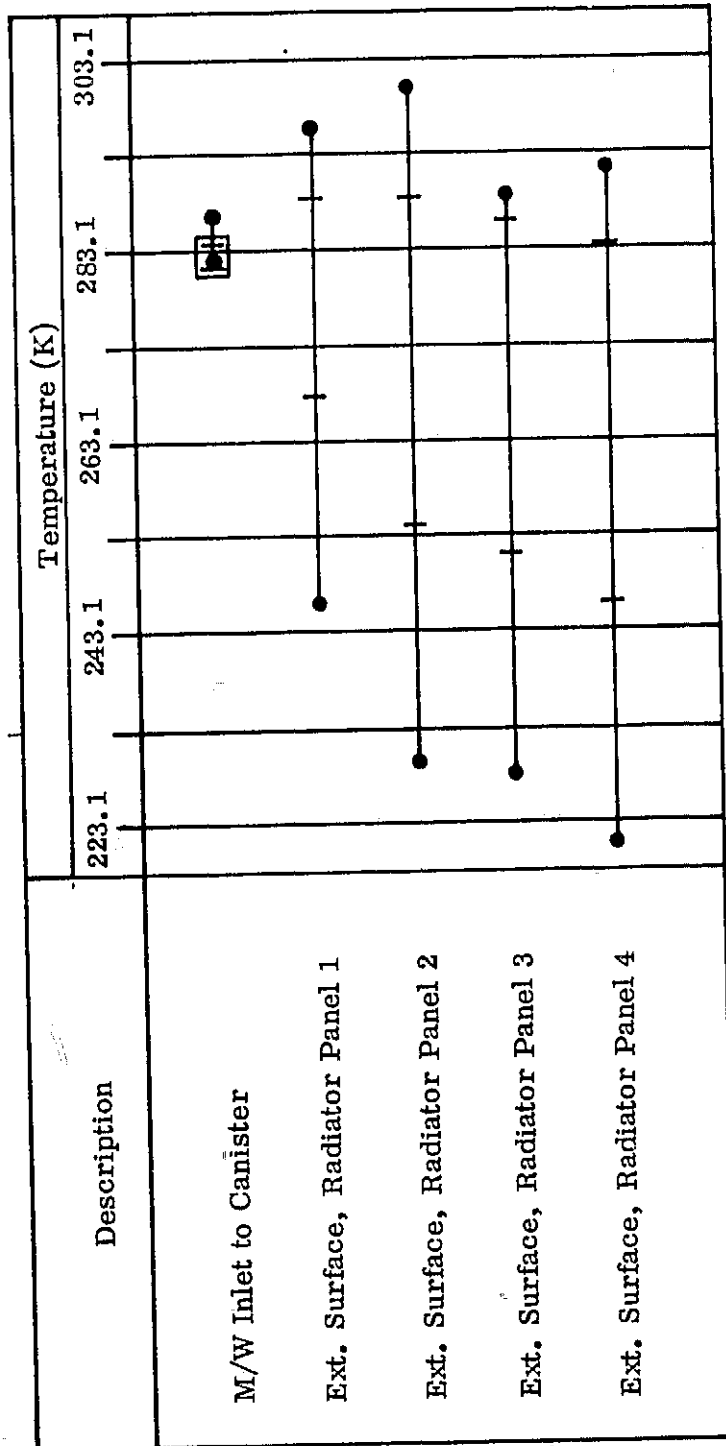
Experiment	Description	Temperature (K)									
		289.2	293.2	297.2	301.2	305.2	309.2				
NRL-A	Case Bottom, MDA End	[Box plot showing temperature distribution for Case Bottom, MDA End]									
	Case Bottom	[Box plot showing temperature distribution for Case Bottom]									
	Case Bottom, Sun End	[Box plot showing temperature distribution for Case Bottom, Sun End]									
NRL-B	Spectrograph Case, Elec. Side	[Box plot showing temperature distribution for Spectrograph Case, Elec. Side]									
	XUV Monitor Case, Side	[Box plot showing temperature distribution for XUV Monitor Case, Side]									
	Spectrograph Case, Elec. Side	[Box plot showing temperature distribution for Spectrograph Case, Elec. Side]									
H-Alpha 1	Front Extension Tube	[Box plot showing temperature distribution for Front Extension Tube]									
	Rear Tube	[Box plot showing temperature distribution for Rear Tube]									
H-Alpha 2	Heat Rejection Window	[Box plot showing temperature distribution for Heat Rejection Window]									
	Main Optics Housing	[Box plot showing temperature distribution for Main Optics Housing]									

TABLE 8. (Continued)

Description	Temperature (K)				
	273.2	281.2	289.2	297.2	
HAO Film Retrieval Door		●	●		
H-Alpha 1 Film Retrieval Door		●	●		
GSFC Film Retrieval Door		●	●		
HCO-A Film Retrieval Door		●	●		
Canister MDA End Plate		●	●		
Canister MDA End Plate		●	●		
Canister MDA End Plate		●	●		
Canister MDA End Plate		●	●		
Canister Sun End Plate		●	●	●	*
Canister Sun End Plate		●	●	●	*
Canister Sun End Plate		●	●	●	
Canister Sun End Plate		●	●	●	
+Y Spar MDA End, Inboard		●	●	●	
+Y Spar Center, Inboard		●	●	●	
+Y Spar Sun End, Inboard		●	●	●	

*Maximum mission temperature exceeded upper measurement limit of 300.1K

TABLE 8. (Concluded)



The liquid TCS performed satisfactorily throughout the mission, operating solely on primary components. Methanol/water flowrate ranged between

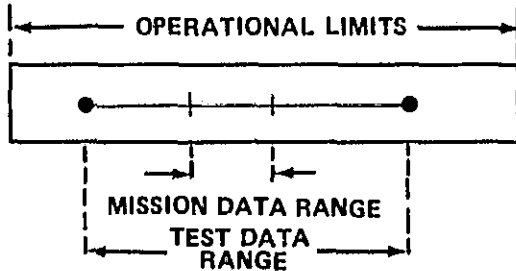


Figure 9. Symbol definition for mission/test temperature tables.

0.122 and 0.127 kg/s and canister cold plate M/W inlet temperature was between 281.95K and 283.70K. Heat absorbed internal to the canister varied from a minimum of approximately 400 watts to a maximum of 610 watts.

Although bounded by test data, flight radiator temperatures were higher than anticipated. For example, maximum radiator panel temperatures during ground test for solar-oriented attitude ranged from 273K to 281K, whereas flight data for the analogous

condition ranged from 283K to 286K. This effectively reduced the system heat rejection capacity from 900 watts to 700 watts. A complete radiator heat flux analysis is contained in Section VII-C. After termination of ATM scientific activities at the end of SL-4, an inflight test was performed to determine the condition of the liquid TCS secondary components which had been inactive during the 9-month mission. The system was activated and performed nominally for approximately 2 hours, thereby demonstrating its storage capability in a space environment. Canister TCS performance data are summarized in Table 9.

Of the measurements chosen for monitoring purposes, only five canister/experiment temperatures violated operational limits during the mission (Table 7). Out-of-limit temperatures were experienced by the H-Alpha 1, H-Alpha 2 and GSFC experiments, primary pitch rate gyro processor, and canister spar. In no case, however, were the ATM's objectives compromised.

B. Rack

During the first 14 mission days, normally-shaded rack zones were exposed to direct solar radiation by attitude maneuvers required to maintain acceptable OW temperatures resulting in several rack components exceeding their allowable temperature limits (see Table 7). After SL-2 crew arrival and parasol deployment, the mission became nominal (vehicle in solar inertial attitude) with off-solar-inertial attitudes for special experimentation requirements causing only transitory temperature extremes. Performance of all thermal control systems was satisfactory and no thermally induced component

TABLE 9. ATM CANISTER TCS ORBITAL PERFORMANCE DATA

System Parameter	Design Requirements		Primary System						Secondary System	
	Min	Max	MD 19			MD 269			Min	Max
			Min	Max	Min	Max	Min	Max		
Canister Inlet Temperature (K)	281.5 ^a	284.8 ^a	282.4	282.9	282.8	283.0	282.9	283.0	282.9	283.0
Canister Inlet to Outlet ΔT (K)	—	2.8 ^a	0.4	1.3	0.5	1.5	0.7	1.4	0.7	1.4
System Flowrate (kg/s)	0.107	—	0.122	0.125	0.121	0.125	0.122	0.124	0.122	0.124
System Pressure (N/m ²)	48 263	131 000	86 184	88 942	86 184	89 632	87 563	88 942	87 563	88 942
Accumulator Level (%)	—	—	74	75	74	75	73	73	73	73
System Heat Load (watts)	—	500	366	452	400	514	452	482	452	482
System Operational Time (hr)	—	5664	—	—	—	6154	—	2	—	2

a. Specification Limits

failures occurred. Maximum and minimum rack temperatures recorded during solar-inertial attitudes are given in Table 10. Mission data are compared with test data and component temperature limits to indicate out-of-limit temperature conditions. Generally, component test temperatures bounded flight temperatures for components. The on/off and proportional component heaters performed as expected, maintaining temperatures within control limits. As a qualitative indication of heat flux ranges experienced in the mission, flight temperatures of a typical thermal cover were compared with thermal vacuum test data (Fig. 10). In the absence of direct flux measurement, thermal cover temperature response gave an approximate indication of flux level. The data selected for comparison indicate minimum and maximum mission flux levels.

As indicated in Table 7, ten rack component out-of-limit temperature conditions occurred because of vehicle off-attitudes and component failures. Out-of-limit temperatures of the primary tape recorder, CBRM, and solar panels were minor. CMG 1 bearing temperature exceeded its upper operational limit when bearing failure occurred on mission day 194 and five rack-mounted rate gyro processors experienced off-scale-high temperatures within a short time following their activation in SL-1. Detailed thermal analysis performed on CMG and rate gyro processor failures are presented in Sections VII-A and VII-B, respectively.

C. Data Correlation

Thermal math model and flight data correlation was performed utilizing rack and canister models (see Section IV-B). These studies consisted of steady-state correlations for mission days 19 and 39 and transient correlations on mission day 105. Mission days 19 and 39 represent orbital β angles of -16 deg and $+70$ deg, respectively. Mission day 19 flight temperature data were fairly stable, indicating relative consistency in experiment and component operation in a fixed environment. Correlation was performed for the last 6 hours in mission day 39, when the earth shadow was negligible. Mission day 105 (β angle 52 deg) transient correlations were of particular interest because the rate gyro processor six-pack had been installed and changes in rack component utilization caused by failures had stabilized. Various environmental conditions were investigated and nominal environmental parameters resulted in the best correlation. Correlation results are summarized as follows:

	<u>Canister Model</u> <u>Percent Correlation $\pm 3K$</u>	<u>Rack Model</u> <u>Percent Correlation $\pm 10K$</u>
MD 19	98	91
MD 39	98	98
MD 105	99	94

TABLE 10. ATM RACK MISSION/TEST DATA COMPARISON

Description	Temperature (K)									
	213.1	233.1	253.1	273.1	293.1	313.1	333.1	353.1	373.1	
<u>Structure and Mechanical Subsystem</u>										
MDA End Mounting Panel					—					
MDA End Mounting Panel					—		—			
Pitch Orbital Lock				—						
Acq Sun Sensor Assy Mfg Plate	•	—			—	•				
<u>Electrical Power Subsystem</u>										
CBRM 1					—					
CBRM 2					—					
CBRM 3				—						
CBRM 4					—					
CBRM 5				—						
CBRM 15			•	—	•					
CBRM 9			•	—		•				
CBRM 10					—		•			
CBRM 11					—		•			
CBRM 12					—		•			
CBRM 13					—		•			
CBRM 14			•	—		•				
CBRM 6			•	—		•				
CBRM 7					—		•			
CBRM 8			•	—		•				
CBRM 16					—		•			
CBRM 17					—		•			
CBRM 18					—		•			

TABLE 10. (Continued)

Description	Temperature (K)								
	213.1	233.1	253.1	273.1	293.1	313.1	333.1	353.1	373.1
<u>Instrumentation and Communication Subsystem</u>									
Remote Analog Submultiplexer 3				■	■				
Remote Digital Multiplexer (M)				●	■	■			
PCM/DDAS					●	■	■		
PCM/DDAS (Redundant)				●	■	■			
Data Storage Interface Unit				●	■	■			
Telemetry Transmitter No. 1				●	■	■			
Telemetry Transmitter No. 2				●	■	■			
Signal Conditioning Rack 6				●	■	■			
Multiplexer Assembly (A1)				●	■	■			
Converter DC to DC					●	■	■		
Signal Conditioning Rack 8				●	■	■			
<u>Attitude and Pointing Control Subsystem</u>									
CMG 1									
Bearing 1						■	■		
Bearing 2						■	■		
Frame				●	■	■			
CMG 2									
Bearing 1						■	■		
Bearing 2						■	■		
Frame				●	■	■			
CMG 3									
Bearing 1						■	■		
Bearing 2						■	■		
Frame				●	■	■			

a. Component Failed During Mission — Subsequently Powered Down.

TABLE 10. (Concluded)

Description	Temperature (K)									
	213.1	233.1	253.1	273.1	293.1	313.1	333.1	353.1	373.1	
CMG Inverter Assembly 1										
CMG Inverter Assembly 2										
CMG Inverter Assembly 3										
Rate Gyro X-1										♦
Rate Gyro X-2										♦-----b
Rate Gyro Y-1										♦
Rate Gyro Y-2										♦-----b
Rate Gyro Z-1										♦-----b
Rate Gyro Z-2										♦-----b
Rate Gyro (Pitch) Secondary										♦
Rate Gyro (Pitch) Primary										♦-----b
Rate Gyro (Yaw) Secondary										♦
Rate Gyro (Yaw) Primary										♦
Pitch Actuator Housing										
Yaw Actuator Housing										
Exp. Pointing Electronic Assembly										
Rate Gyro Y-3										♦-----b
Digital Computer										
Roll Actuator Housing										
Rate Gyro X-3										♦
Workshop Computer Interface Unit										
Rate Gyro Z-3										♦

b. Heater Failure — Temperature Above Instrumentation Limit.

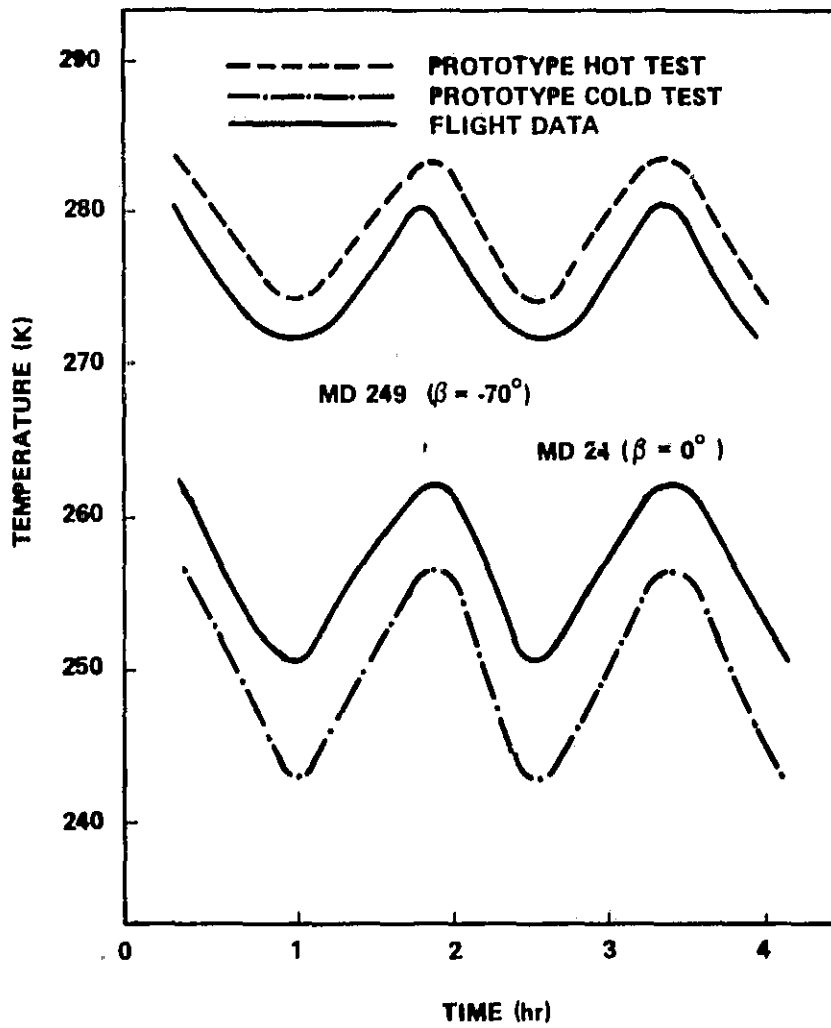


Figure 10. Typical thermal cover temperature response.

1. Canister Model. Steady-state canister analysis, utilized as initial conditions for one-orbit transient simulations, were acceptable with no major discrepancies observed between results and earlier correlation efforts. Boundary conditions utilized for the correlation analyses were component powers, experiment TCS powers and setpoint temperatures, solar flux, and sun shield solar absorptivity. Deviations between analysis and flight data have been statistically analyzed, together with similar results obtained for prototype and flight thermal vacuum tests, and are summarized as follows:

Normal Distribution Parameter	Prototype T/V Test		Flight T/V Test	Mission	
	Cold	Hot	Cold	MD 19 (Cold)	MD 39 (Hot)
Mean Temperature Difference (K)	-0.2	-0.5	0.3	-0.2	-0.3
Standard Deviation	1.2	1.4	1.4	1.1	1.2

Ninety-eight percent of all canister temperature measurements correlated within $\pm 3K$ for both mission days. Typical statistical correlation distribution analysis results are presented in Figure 11.

Transient canister model data correlations for the eight experiments were acceptable and compared favorably with previous correlation studies. Flight conditions were simulated for one orbit on mission day 105. Ninety-nine percent of all canister temperature measurements correlated within $\pm 3K$.

2. Rack Model. Steady-state rack model data correlation compared favorably statistically with previous correlation efforts. The flight data presented in the correlation are average values for the days considered. Boundary conditions include temperatures (canister MDA end-plate and gyro housings), component power dissipations, and environmental absorbed fluxes. Since on/off heater operation cannot be simulated in a steady-state analysis, component temperatures are average values. The temperature differences for mission days 19 and 39 are statistically analyzed and summarized along with prototype test correlation results on the next page.

Normal Distribution Parameter	Prototype T/V Test ¹		Mission	
	Cold	Hot	MD 19 (Cold)	MD 39 (Hot)
Mean Temperature Difference (K)	0.9	-0.1	-3.1	-0.3
Standard Deviation	5.1	4.6	5.1	4.6

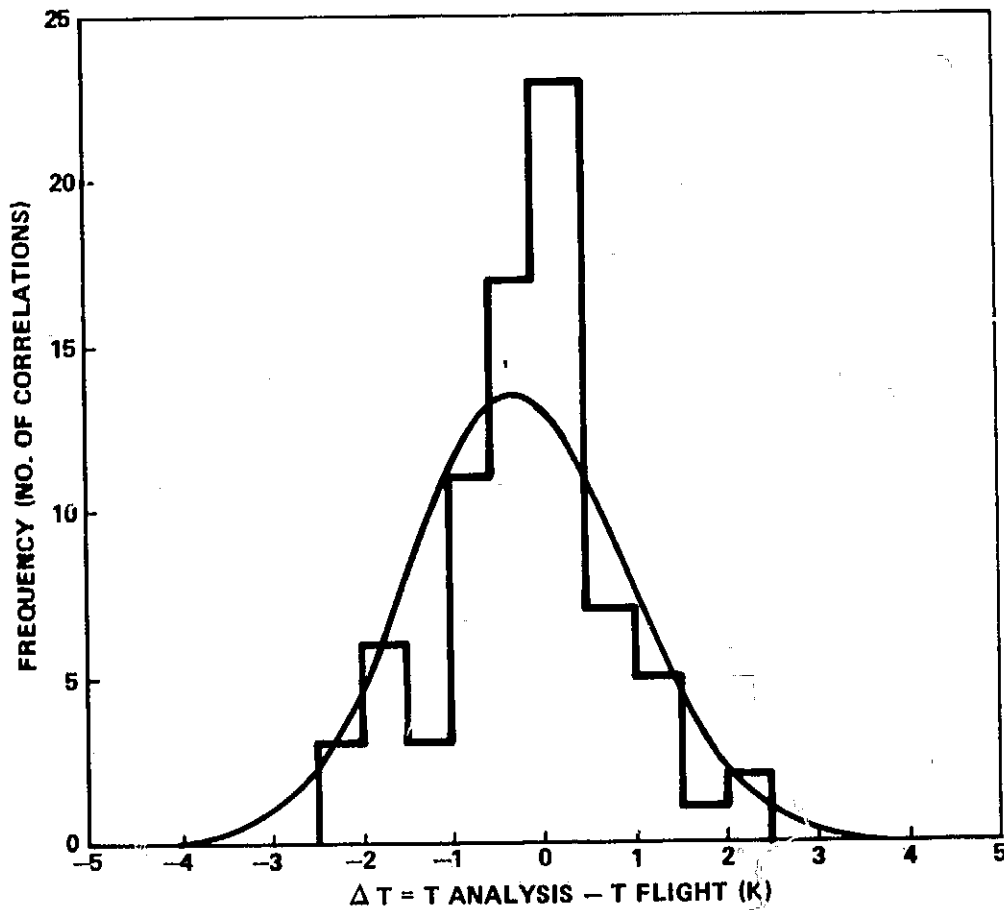


Figure 11. Canister correlation analysis for MD 39.

1. Steady-state testing not conducted on flight vehicle.

Transient data correlation of rack components was made for mission day 105. Since the six-pack replacement gyros were installed, only three rack gyros (X-1, Y-1, and Z-3) remained operative. Sixty percent of the 65 measurements correlated were within $\pm 5K$ and 94 percent were within $\pm 10K$. Overall, the results obtained in the correlation were satisfactory.

VII. OFF-NOMINAL CONDITIONS

ATM thermal design performed satisfactorily throughout the mission, although several out-of-limit temperature conditions occurred. However, equipment failures, changes in anticipated performance ranges, and variations in operational procedures required thermal analysis support. Thermally related off-nominal conditions are discussed in the following sections.

A. Control Moment Gyro

SkyLab used three CMGs to stabilize and control vehicle attitude. Each CMG contained a 0.56 m diameter, 68.03 kg wheel that rotated at approximately 9000 revolutions per minute. The wheel motor, rotor, and axle were supported by two ball bearing assemblies. Centrifugal force acting upon an oil saturated nut assembly attached to the rotating shaft provided bearing lubrication through fixed metering orifices. Bearing heaters maintained temperatures at nominal values. A parameter of particular significance was the temperature difference between inner and outer bearing race because increased temperature differences resulted in reduction of radial bearing clearance. For nominal clearance, bearing temperature differences greater than 45K were critical.

The CMG flight failure occurred during a loss of signal (LOS) period when only the motor current was recorded. Prior to LOS, bearing cartridge temperature (case surrounding outer race) was reading 294.8K and the bearing heaters had stopped cycling due to the high β angle on mission day 194. At next acquisition of signal (AOS), indicated wheel speed was 0 and the number 1 bearing cartridge temperature was 356.5K. The electrical induction wheel brake was applied approximately 7 min after AOS. The onboard computer did not signal CMG auto shutdown which would occur if the bearing cartridge temperature had exceeded 366.5K. The CMG thermal model predicted that, if the wheel had stopped during LOS, the bearing cartridge would have exceeded the 366.5K shutdown limit. Therefore, it was assumed that the speed sensor had been damaged and the wheel was still spinning at AOS. From the recorded current data and motor torque curve, wheel speed and kinetic energy were

derived and used as input to the thermal model. All energy from the wheel deceleration was applied as heat input to number 1 bearing and was divided equally between inner and outer bearing races. The analysis showed that the wheel speed was approximately 4700 revolutions per minute at the time the induction brake was applied. The resulting bearing cartridge temperature compared to flight data along with the predicted race-to-race temperature difference are shown in Figure 12.

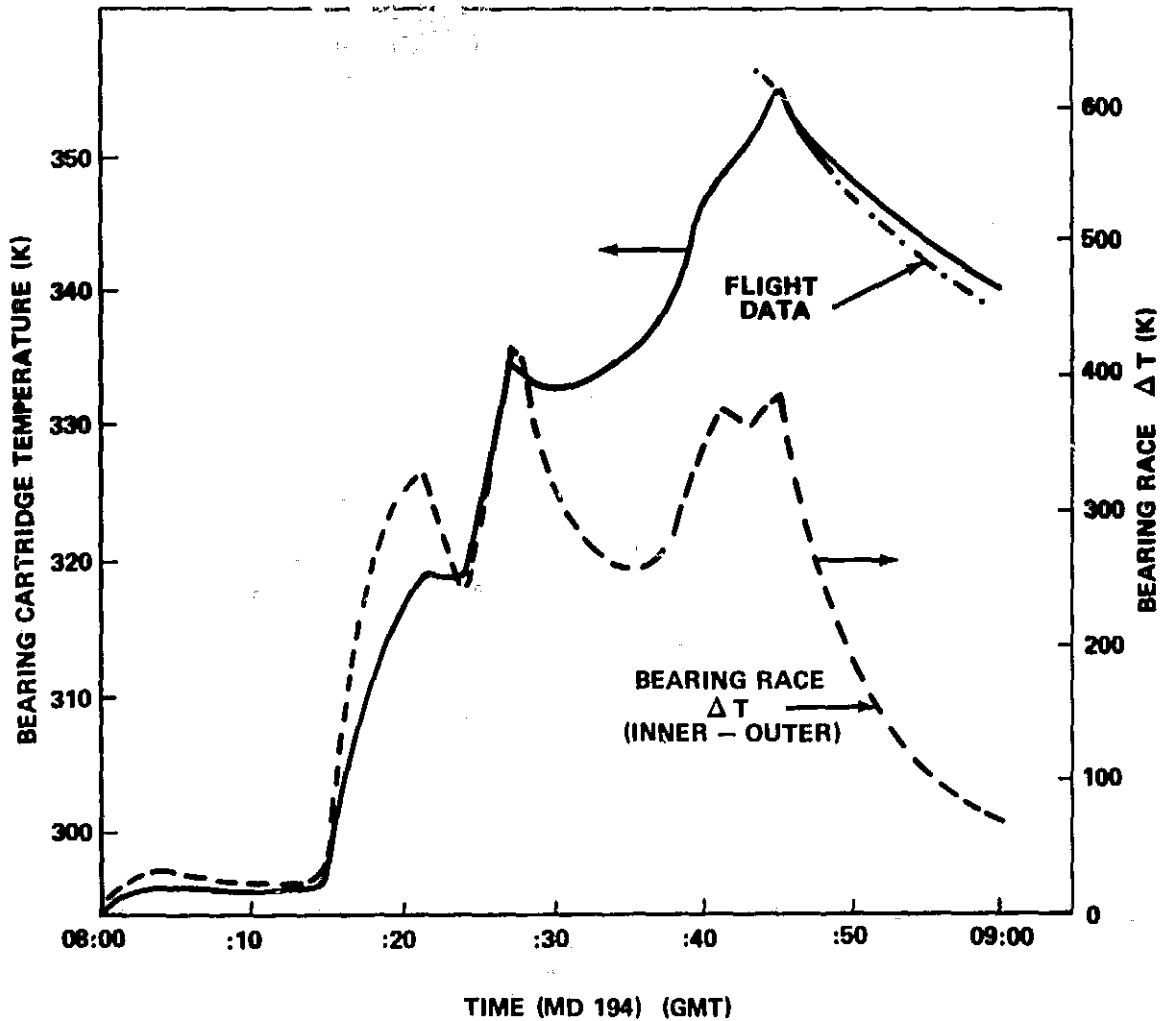


Figure 12. Predicted bearing temperatures during CMG number 1 failure.

Good correlation with flight data was achieved but flight temperatures peaked earlier at higher temperatures than predicted by the model. Inaccuracies were probably caused by current-to-speed conversion calculations and physical changes in the bearing and its thermal properties after failure. The predictions showed that, on MD 194 at 08:15 GMT, number 1 bearing race-to-race temperature difference was great enough to cause loss of radial clearance, resulting in bearing failure.

Thermal math model temperature results for the flight CMG bearing failure supported the contention that increased bearing friction (causes unidentified) resulted in excessive heating and subsequent reduction in bearing clearance, ending in bearing failure. Increased bearing friction may have resulted from mechanical changes in the bearing or insufficient lubrication.

B. Rate Gyros

The rate gyro processors (RGP) were inertial sensors used to provide rate information for Skylab attitude control. Nine rack RGPs, three for each principal axis, provide rate information for the overall Skylab attitude control and four canister RGPs in the canister provided rate information for fine pointing of experiments. The gyro was enclosed in a fluid-filled assembly which mounted to the processor case. The gyro fluid was maintained at $340.96\text{K} \pm 1\text{K}$ by a 21.9 watt heater operated by a pulse-width proportional controller.

Five rate gyros on the rack (i. e., X-2, Y-2, Y-3, Z-1, and Z-2) and one in the canister (primary pitch) experienced temperature problems during SL-1/SL-2. This problem was manifested as off-scale-high temperature readings for the gyro. Since the telemetered temperature range was 335K to 346K, the temperature was in excess of 346K. In all cases, the gyro heaters appeared to control for a period of time following activation and warmup. Subsequently, a sharp temperature increase was noted. Figure 13 shows the temperature history (typical of all gyros) for the rack-mounted Y-2 rate gyro. Mounting panel temperature data indicated a nominal conductive and radiant thermal sink. Also, the pitch primary gyro, located inside the temperature controlled canister, showed a similar thermal anomaly, thus eliminating external environment effects as a possible failure cause. The electronics and gyro motor power dissipations were insufficient to cause the rapid RGP heating. Therefore, test and analytical efforts concentrated on investigating gyro performance with full-on gyro heaters.

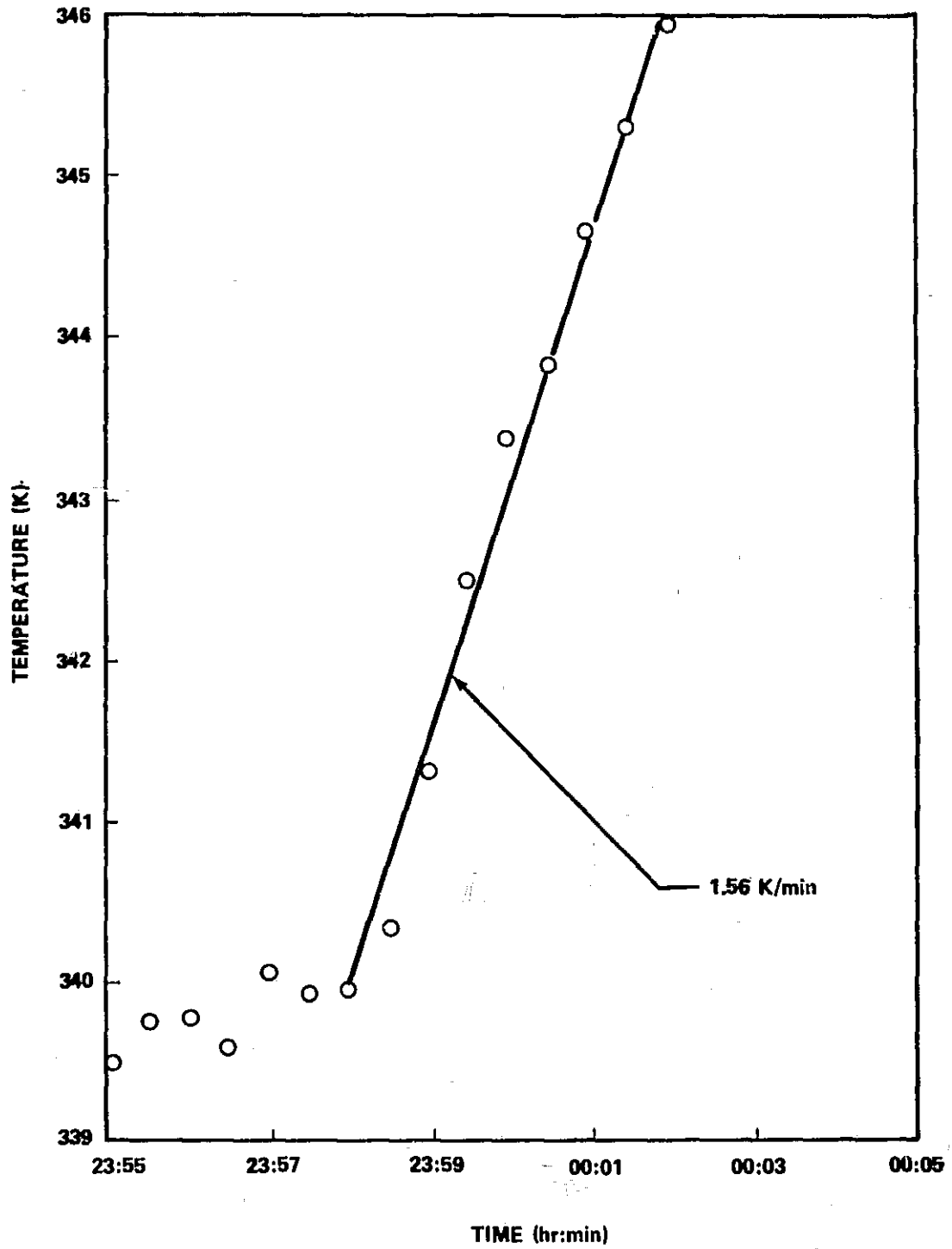


Figure 13. Y-2 rate gyro over-temperature transients.

Thermal testing, with supplementary instrumentation, and thermal analyses results provided detailed temperature distribution data. Steady-state thermal tests of extreme conditions identified maximum gyro temperatures as a function of various parameters. Transient RGP tests were performed to determine gyro warmup characteristics from ambient to normal operating temperature (340.96K) and to determine the rate of temperature increase following a full-on heater circuit failure. Subsequently, inflight testing was performed on the Z-1, X-2, and Y-3 gyros. Analytical data, compared with test data in Figure 14 for a failed heater, predicted a maximum temperature of 395K for any failed gyros. Through extensive analyses and ground tests, the cause of the RGP temperature anomaly was proven to be a design deficiency that allowed loosening of a power switching transistor from its heat sink rail. Loosening of the transistor mounting allowed the transistor to thermally saturate and leak excessive current to the gyro heater, resulting in an uncontrolled heater.

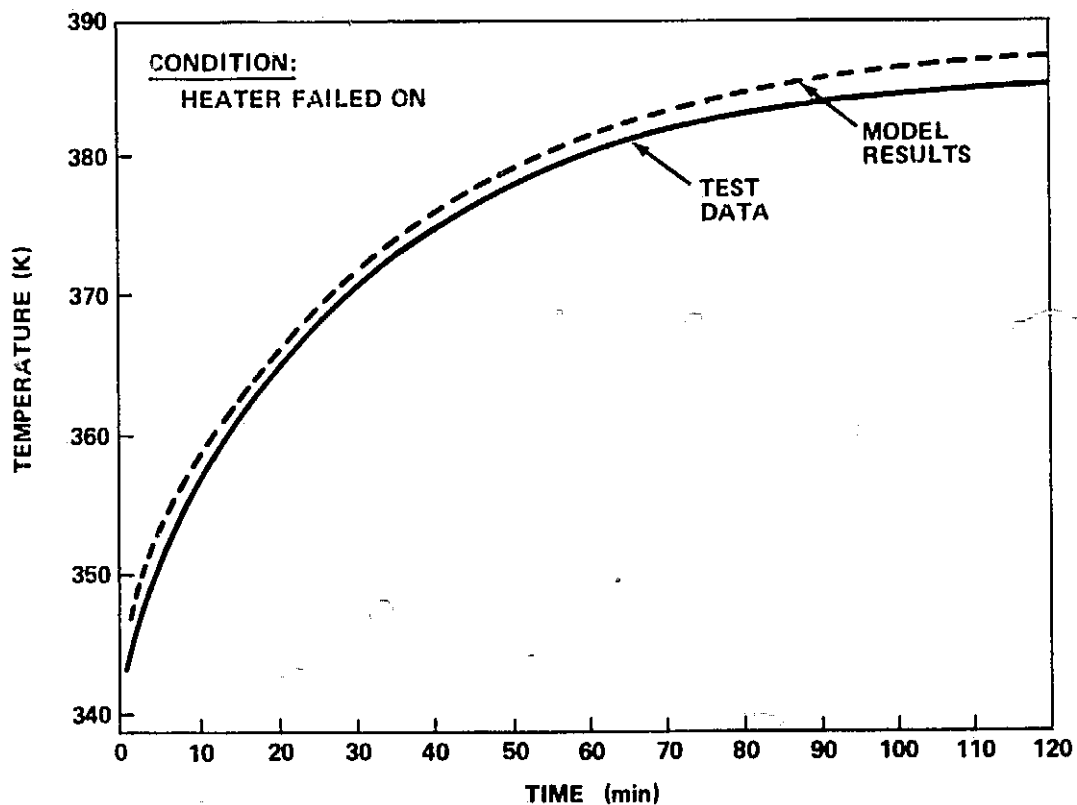


Figure 14. Rate gyro thermal model/test data correlation.

A backup assembly of six RGPs (six-pack) was constructed, carried to Skylab by the SL-3 crew, installed in the MDA, and patched into the attitude and pointing control system. None of the RGPs in the six-pack exhibited abnormal drift rates.

C. Canister TCS Radiator

During the second high β angle period (full-sun condition) of SL-4, the canister TCS (Fig. 5) radiator coolant flowrate approached 100 percent, indicating that maximum heat rejection capability had been achieved. This condition was not anticipated from ground tests and analyses.

Degradation in radiator coating solar absorptivity was investigated. The analysis revealed a gradual increase in radiator flux, as shown in Figure 15. Average increase over the Skylab mission was 7 percent. Most of this increase is attributed to solar constant seasonal variation which increased solar flux 5 percent during the mission. Therefore, it was concluded that the radiator coating did not appreciably degrade.

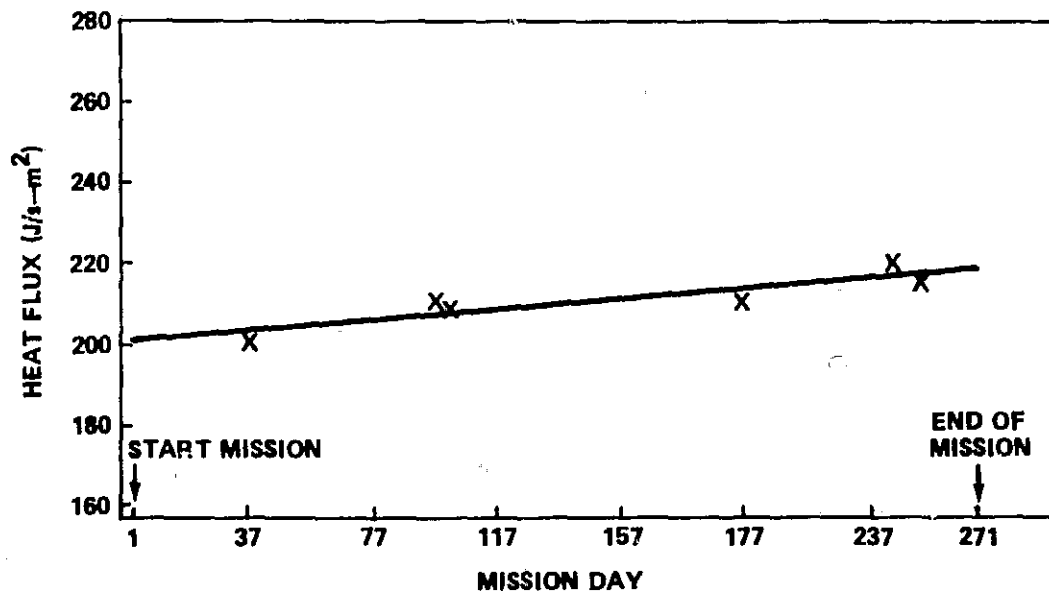


Figure 15. Average absorbed radiator heat flux versus mission day.

The average absorbed radiator heat flux during the mission was calculated from measured temperature data and compared to predicted fluxes (Fig. 16). The flight data correlates closely with hot case predictions except at maximum β angles where actual fluxes exceed predicted fluxes by approximately 19 per cent.

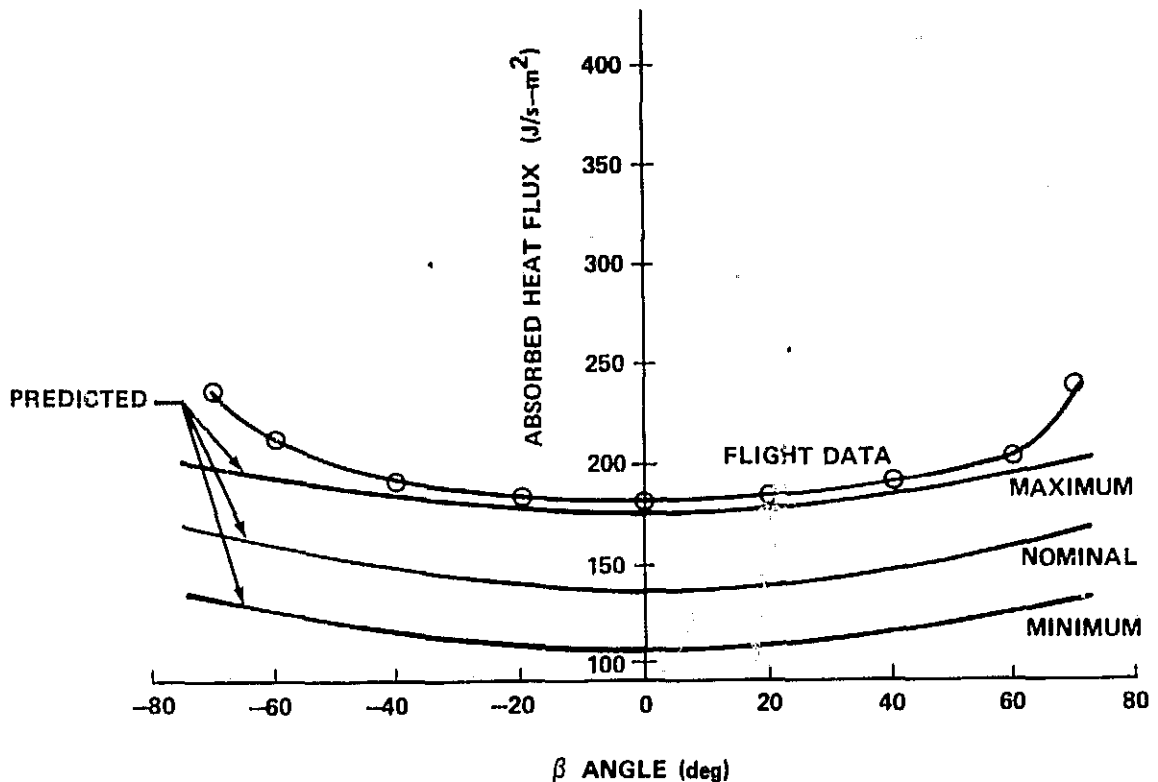


Figure 16. Predicted/flight radiator average absorbed heat flux.

The analysis demonstrated that radiator external environmental fluxes experienced during high β angles were in excess of those predicted using a detailed computer model. This situation served to reduce the overall TCS heat rejection capability; however, the extra margin inherent in the system design maintained acceptable experiment thermal conditions.

D. Solar Shield Absorptivity Degradation

During the SL-3 mission, temperature data indicated that the thermal control coating on the canister solar shield was degrading beyond anticipated levels. During SL-4 the solar shield reached an equilibrium temperature of approximately 353K, resulting in high canister heat loads which contributed to several minor out-of-limit temperature conditions. An analysis was performed to determine degradation as a function of solar exposure time. In addition, postmission solar absorptivity measurements were taken on a 10.2 cm (4 in.) diameter circular cover affixed to the solar shield that was retrieved by the SL-4 crew.

The ATM solar shield was coated with S-13G white paint having a nominal solar absorptivity at application of 0.20 and an infrared emissivity of 0.9. Prior to the mission, ground testing indicated that solar absorptivity increased with exposure to ultraviolet radiation. Although there was significant variation in results, data showed a maximum absorptivity change of 0.1, stabilizing between 3000 and 4000 equivalent solar hours exposure. Consequently, it was anticipated that absorptivity would not increase beyond 0.30 during the mission.

Utilizing the temperature transducer located on the solar shield, values for α_s were calculated for the mission. The analysis assumed the shield was an adiabatic surface since heat leak through the shield was calculated to be less than 3 percent of total absorbed heat. The solar constant utilized for analysis was 1353 J/s-m², adjusted for seasonal variation. Earth infrared flux and albedo, analytically computed, indicated negligible values for earth albedo flux. Since the shield was alternately exposed to full sun and earth shadow, except at β angles greater than 69 deg, care was taken to record shield temperatures only when equilibrium conditions had been achieved. Analytical results, an averaged measured value for the 10.2 cm (4 in.) circular cover and premission ground test data are compared in Figure 17. At mission termination (approximately 4320 hours solar exposure), midrange values of α_s were 0.53 from analysis and 0.46 from the circular cover measurement. Both values exceed the nominal prediction of 0.30 based on premission test data.

Initially, increased degradation was thought to be attributable to surface contaminants. Results from sun shield mounted quartz crystal microbalances tend to contradict this conclusion. This source indicated negligible contaminant deposition on the sun side of the solar shield. Another possible explanation for unanticipated degradation was that ground tests did not employ accurate simulation of solar exposure. In particular, it is possible that effects caused by other than ultraviolet radiation were not accounted for and/or that computation of equivalent solar hours based on shorter periods at multiple solar constants may not be valid.

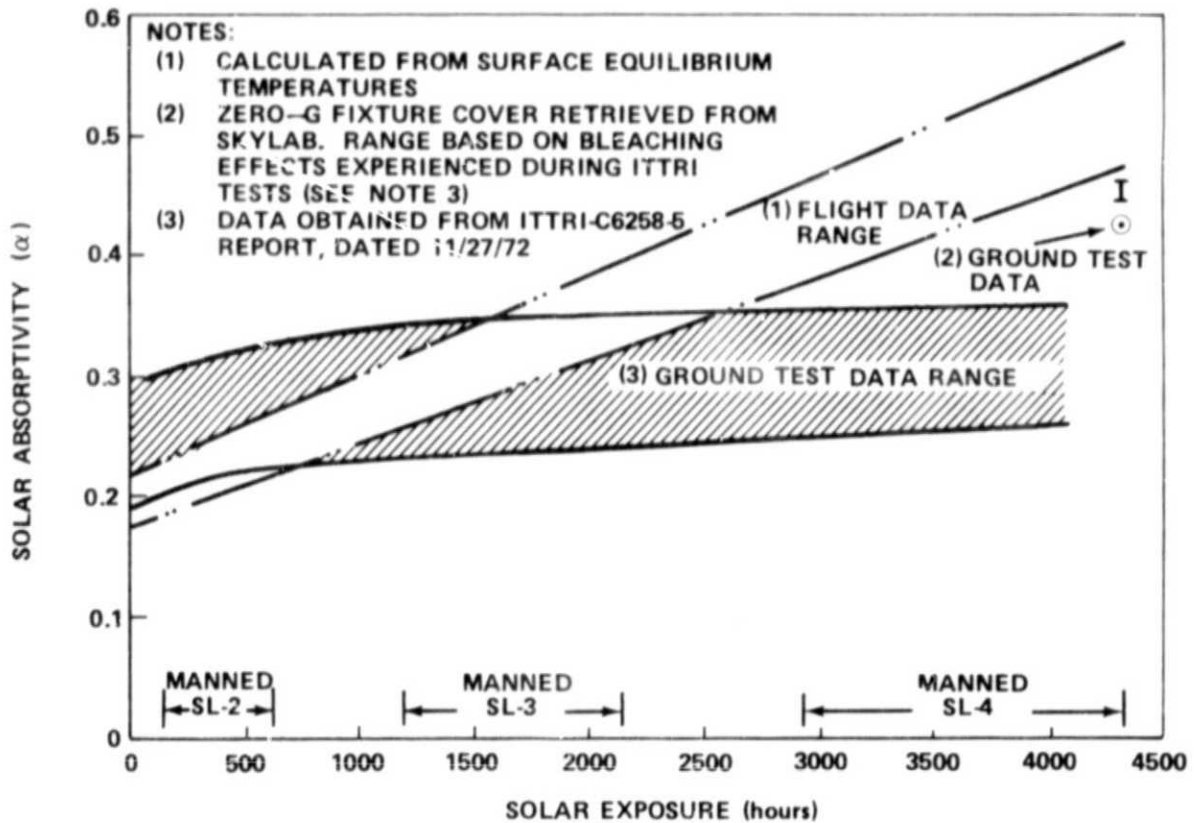


Figure 17. ATM canister solar shield solar absorptivity degradation.

E. Canister Pressure

Pressure within the canister below 10^{-3} N/m² was required to avoid electrical arcing in experiment high-voltage components. For several days after SL-1 launch, canister pressure decayed at a slower rate than expected with intermittent pressure spikes. The canister internal pressure profiles after SL-1 launch is presented in Figure 18.

It was concluded that the cold cathode vacuum gauge was correct and that pressure spikes were a result of outgassing internal to the canister since positive correlations with external gas sources (e.g., workshop venting) could not be made. Data from ground tests on the multilayer insulation similar to that used within the canister supported the postulation that insulation can outgas in bursts resulting in pressure spikes as recorded in the canister during flight. The outgassing was probably due to water vapor trapped in the insulation.

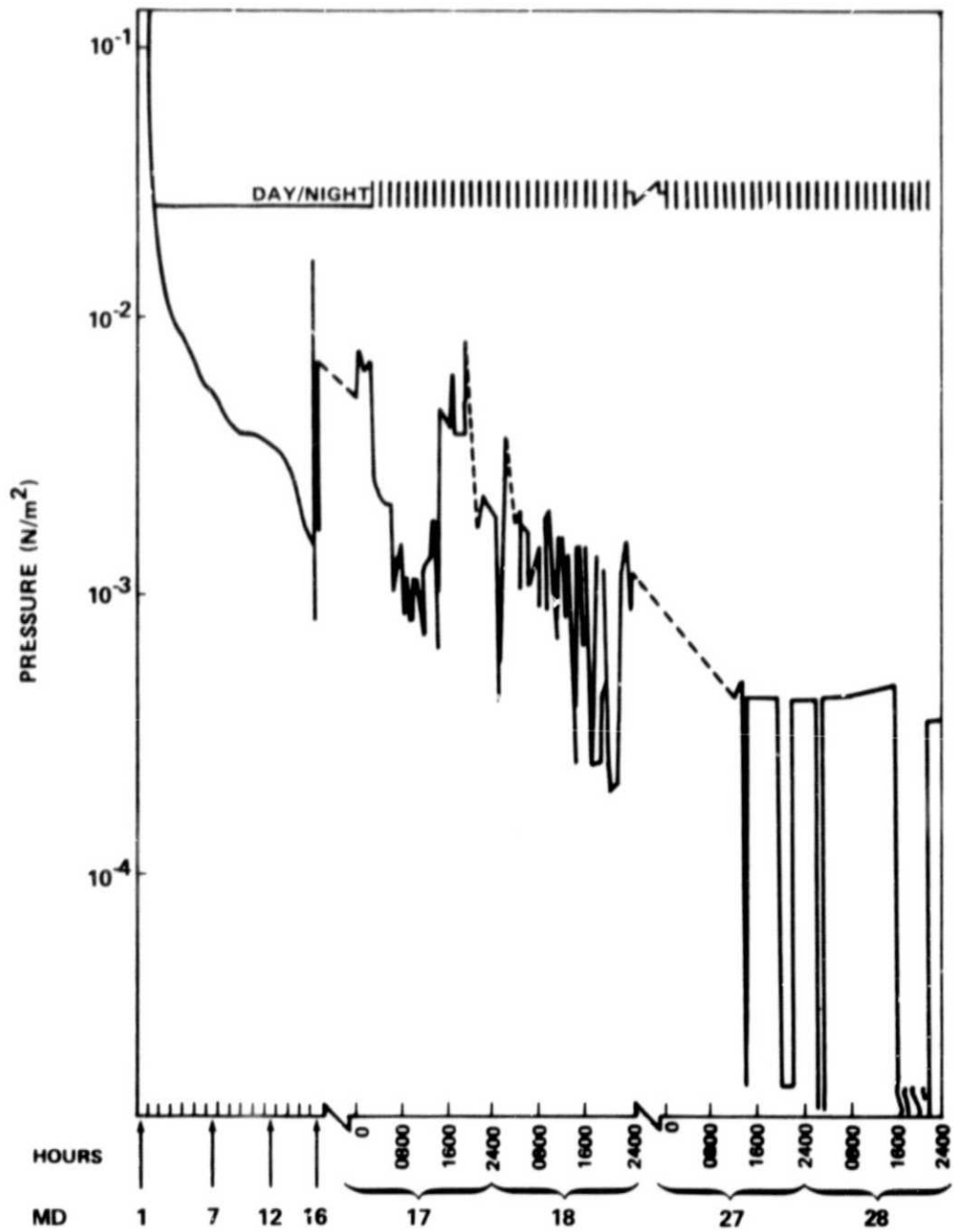


Figure 18. Canister internal pressure profile after SL-1 launch.

F. Other Out-of-Limit Conditions

In addition to previously discussed off-nominal conditions, several other minor out-of-limit conditions occurred during the mission. Although out-of-limit excursions were minor and insignificant, as to hardware functional operation, it does point out that worst-case premission design parameters are sometimes exceeded during a mission. Out-of-limit temperature conditions associated with the solar array, film cameras, and experiments are discussed in the following paragraphs.

During off-solar attitude maneuvering to maintain OW temperatures within acceptable limits following loss of the meteoroid shield, out-of-limit low temperatures were observed for the ATM solar array. Low solar array thermal capacitance required that the array be solar oriented prior to entering the earth shadow to prevent excessively cold array temperatures during the shadow period. Maneuvers which prevented solar heating caused the array to exceed its lower temperature limit by approximately 7K, resulting in a possible decrease in electrical circuit reliability. Therefore, the degradation noted in solar array performance may have been partially caused by the above-mentioned maneuvers (see NASA TM X-64818).

Six experiments utilized film cameras with removable film magazines which were replaced with unexposed film magazines during astronaut EVA. This replacement required that film magazines be temporarily stored in the relatively warm environment of the fixed airlock shroud (FAS) on the Airlock Module. Since maximum allowable film temperature changes had to be maintained within approximately 14K, storage time in the FAS had to be limited. Premission analysis, based on EVA timelines, indicated acceptable film temperatures. However, during the second EVA of SL-3, FAS storage time of the AS&E film was prolonged. Postmission analysis using flight boundary conditions indicated that film retrieved from the ATM exceeded its upper temperature limit by approximately 2K.

Out-of-limit temperatures were experienced by H-Alpha 1 and H-Alpha 2 experiments. Both experiments utilize passive thermal control by employing gold-coated main tubes which house the telescopes' optical elements. Therefore, the experiments relied on balancing of internally-dissipated heat and external radiation to maintain correct main tube temperatures. However, during the mission H-Alpha vidicons were deactivated for functional reasons during non-data-taking modes, resulting in both main tubes dropping approximately 2.5K below their lower temperature limits. The main tubes operated within temperature limits whenever vidicons were activated.

The GSFC mirror exceeded its maximum temperature limit when unexpected warm internal canister temperatures resulted from degraded thermal coatings on the solar shield (see Section D) and GSFC aperture plate. The proximity of the mirror to the aperture plate and canister sun end made it sensitive to temperatures of these surfaces. Also, the warm biased mirror assembly's design resulted in a very small tolerable heat load margin.

VIII. CONCLUSIONS

A. System Performance

Overall satisfactory ATM thermal performance throughout the Skylab mission supports the general approach taken in obtaining a workable thermal design. No thermal design inadequacies were identified nor were there any thermally induced equipment failures. With few exceptions, ATM's thermal performance remained within acceptable temperature limits although the vehicle was oriented in orbital attitudes exceeding design specifications. Temperature data show that no temperatures seriously violated allowable limits during the mission until after component failures had occurred. The minor out-of-limit temperature conditions were attributed to off-attitude orientations, thermal control coating degradation, and equipment operational changes. However, none of these out-of-limit temperatures seriously impacted operations or objectives. The only off-nominal thermal control condition during the mission was the degradation rate of S-13G paint on the solar shield. Although this caused several minor out-of-limit temperatures late in the mission, the conditions had no significant impact. The results of correlating mission and analytical data verified that thermal models were able to predict flight temperatures. The analysis indicated that 98 percent of calculated canister temperatures correlated within $\pm 3K$ of mission data and 91 percent of calculated rack temperatures correlated within $\pm 10K$ of mission data.

B. Future Program Applications

From inception through conclusion of the Skylab program, various events occurred that were significant and warrant enumeration for possible benefit to future programs. The following discussion covers items from ATM thermal design through development and flight.

Utilizing multilayer insulation in enclosed areas where low orbital pressure ($< 10^{-3}$ N/m²) are required should be avoided if possible. Although canister internal insulation was protected and purged through all ground operations, the insulation outgassed 14 days in orbit before canister pressure stabilized below 10^{-3} N/m².

System thermal designs should maintain sufficient margins to allow for modeling errors and unexpected mission contingencies by utilizing $\pm 3 \sigma$ environmental deviations, degraded thermal coatings, and maximum heat dissipation dispersions in the analyses. This design philosophy, utilized for ATM, resulted in a thermal control system capable of maintaining acceptable temperatures under adverse flight conditions such as those which occurred when the OW meteoroid shield failed.

Incorporation of several experiments, each from a separate source, into an integrated thermal design requires simple, well defined thermal interfaces between experiments and vehicle thermal control system. By establishing simple, well defined thermal interfaces, all thermal design efforts can be simultaneously performed with clear definition of responsibility. Therefore, changes in one experiment's design requirements do not significantly perturbate other thermal designs, thus minimizing design changes and cost. Also, specified thermal data of not only experiments but all components should be generated during hardware development, qualification, and acceptance testing. During the ATM program, thermal design engineers were continually handicapped by insufficient thermal data; consequently, good system thermal analyses were not generated until late in the program.

Thermal design engineers should be required to perform frequent visual vehicle status and configuration checks from start of assembly through launch operations. These types of inspections were performed during the ATM program and revealed numerous hardware discrepancies which could have resulted in flight thermal problems. Such items as incorrect paint and paint patterns, dirty thermal control surfaces, poor and/or improper insulation installation, and incorrect thermal mounting of components were discovered.

Any mechanical-electrical thermal control system used in thermal design should be breadboard-tested prior to vehicle installation. Schedule incompatibilities did not allow this in the ATM program and an instability was discovered during the first full-scale thermal vacuum test. Thermal modeling of such a system cannot account for system mechanical characteristics and only simulates electrical logic "as designed" rather than "as built."

Full-scale vehicle thermal vacuum testing should be performed if possible. Vehicle testing under maximum and minimum predicted orbital thermal conditions should be planned to force any design weaknesses (if they exist) so that potential failure points, as well as the type of failures, are known. In each successive ATM test, additional design deficiencies were discovered which could have resulted in flight difficulties. In addition, ATM thermal characteristics were well defined by test data and, consequently, adverse flight conditions resulting from the OWS meteoroid shield failure were rapidly evaluated by thermal personnel.

The vehicle should have a thermal control system (e.g., purge) for vehicle checkout on the launch pad. ATM was to have no "on pad" checkout; however, due to a lightning strike several systems required retesting. The unavailability of "on pad" vehicle thermal control in a fully powered condition limited these checkouts in time and scope.

IX. SUPPLEMENTARY DOCUMENTS

1. TMX-64808, MSFC Skylab Final Program Report.
2. TMX-64809, MSFC Skylab Corollary Experiments Final Technical Report.
3. TMX-64810, MSFC Skylab Airlock Module Final Technical Report.
4. TMX-64811, MSFC Skylab Apollo Telescope Mount Final Technical Report.
5. TMX-64812, MSFC Skylab Multiple Docking Adapter Final Technical Report.
6. TMX-64813, MSFC Skylab Orbital Workshop Final Technical Report.
7. TMX-64814, Skylab Mission Report-Saturn Workshop.
8. TMX-64815, MSFC Skylab Apollo Telescope Mount Summary Mission Report.
9. TMX-64816, MSFC Skylab Mission Sequence Evaluation Report.
10. TMX-64817, MSFC Skylab Attitude and Pointing Control System Mission Evaluation Report.
11. TMX-64818, MSFC Skylab Electrical Power System Mission Evaluation Report.
12. TMX-64819, MSFC Skylab Instrumentation and Communication System Mission Evaluation Report.
13. TMX-64820, MSFC Skylab Corollary Experiments Systems Mission Evaluation Report.
14. TMX-64821, MSFC Skylab Apollo Telescope Mount Experiment Systems Mission Evaluation Report.

15. **TMX-64822, MSFC Skylab Thermal and Environmental Control System Mission Evaluation Report.**
16. **TMX-64824, MSFC Skylab Structures and Mechanical Systems Mission Evaluation Report.**
17. **TMX-64825, MSFC Skylab Crew Systems Mission Evaluation Report.**
18. **TMX-64826, MSFC Skylab Contamination Control Systems Mission Evaluation Report.**

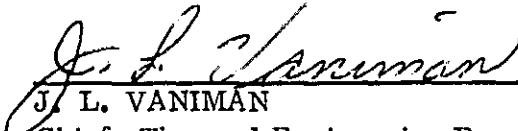
APPROVAL

MSFC SKYLAB APOLLO TELESCOPE MOUNT THERMAL CONTROL SYSTEM MISSION EVALUATION

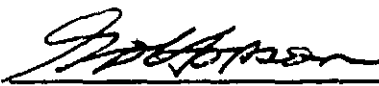
By Uwe Hueter

The information in this report has been reviewed for security classification. Review of any information concerning Department of Defense or Atomic Energy Commission programs has been made by the MSFC Security Classification Officer. This report, in its entirety, has been determined to be unclassified.


This document has also been reviewed and approved for technical accuracy.



J. L. VANIMAN
Chief, Thermal Engineering Branch



G. D. HOPSON
Chief, Engineering Analysis Division



R. ISE SEP 9 1974
Manager, Skylab Program Office